

# Modelling the Vulcanization Reaction of Devulcanized Rubber

by

**Ankita Saikia**

A thesis  
presented to the University of Waterloo  
in fulfillment of the  
thesis requirement for the degree of  
Master of Applied Science  
in  
Chemical Engineering

Waterloo, Ontario, Canada, 2014

©Ankita Saikia 2014

## **AUTHOR'S DECLARATION**

I hereby declare that I am the sole author of this thesis. This is a true copy of the thesis, including any required final revisions, as accepted by my examiners.

I understand that my thesis may be made electronically available to the public.

## **Abstract**

The generation of scrap tires/rubber is increasing annually and thus there is a need for a safer and more efficient method of disposal or reuse of this rubber. As the direct disposal (burning/ land filling) of scrap rubber has harmful effects on the environment, recycling and reusing is given great consideration. For reusing, scarp rubber can be devulcanized and used in many applications. Some methods for devulcanization of rubber have been developed and devulcanized rubber can be blended with virgin rubber and re-cured.

However, the curing behavior of devulcanized rubber will vary compared to that of virgin rubber so it would be helpful if a proper model could be obtained in order to characterize and optimize the curing properties of devulcanized rubber with respect to the curatives added.

The main objective of this study is to characterize the vulcanization reaction of devulcanized rubber by using a kinetic model which will help in predicting the kinetics of vulcanization with change in temperature and the amount of curatives added. Also, it will help to obtain a better understanding of the relationship between curing behavior and properties of devulcanized rubber. It may further help in minimizing the time required for choosing the appropriate cure system for compounds involving devulcanized rubber.

This study involves fitting the cure kinetic reaction model on differential scanning calorimetry (DSC) data. Vulcanization is an exothermic process in which the energy released during the reaction is assumed to be proportional to the bonds formed and thus can be related to the degree of vulcanization. DSC records this heat released which is later used to calculate the reaction rate and degree of cure.

As vulcanization is a chemical process, its simulation involves characterization of kinetic parameters. Experiments have been done using 7 different samples of devulcanized rubber which vary in curative composition. Those samples have been tested using DSC at different temperature scanning rates and a kinetic model was used to fit the DSC data and to determine the kinetic model parameters. The Kissinger model along with the Arrhenius equation was used to determine the vulcanization activation energy and the Kamal-Sourour model was used to fit the data obtained from DSC through non-linear least square techniques and estimate the rest of the parameters.

To have a comparison between virgin rubber and devulcanized rubber, natural rubber samples with similar formulations have been mixed and tested in the same way. Also, to further investigate the cure kinetics of devulcanized rubber, blends of virgin rubber (tire tread compound) with different amounts of devulcanized rubber were analyzed in similar ways.

## Acknowledgements

I would like to express my gratitude to my supervisor Prof. Costas Tzoganakis for giving me this opportunity to fulfill one of my most desired ambitions of pursuing higher education in the field of rubber technology. I would also like to thank him for his continuous support and guidance throughout my study.

I am thankful to Dr. Alex Penlidis and Dr. Neil McManus, my committee members, for accepting to be readers of my thesis by taking out time from their busy schedule.

Also, my sincere regards to Dr. Juan Pablo Hernandez-Ortiz and Nora Catalina Restrepo for sharing their work on modelling which gave me a clear idea in order to carry out my work. Again a special thanks to Nora Catalina Restrepo for being patient with me and my doubts.

Further, I would like to acknowledge the continuous support and assistance of my friend and colleague, Prashant Mutayala. Also, thanks to my colleagues, Dr. Shuhan Zhu and Dr. Mohammad Meysami for their help and guidance.

I would also take this opportunity to thank my family in Canada, Momba, Jason, D and M, for their strong moral support and love, without which I may not have been able to come so far from home to pursue my studies. Loads of thanks to my family back in India for their love.

My dear friends- Ashish, Bhushan, Chelsea, Joshi, Khushboo, Sania, Swati and Tamara thanks for standing by me and making things easy for me.

## **Dedication**

To my brother, *Anirban Saikia...*

## Table of Contents

AUTHOR'S DECLARATION.....	ii
Abstract.....	iii
Acknowledgements .....	v
Dedication.....	vi
Table of Contents .....	vii
List of Figures .....	ix
List of Tables .....	xi
List of Abbreviations and Symbols .....	xiii
Chapter 1 Introduction.....	1
1.1 Motivation.....	1
1.2 Research Objectives.....	2
1.3 Thesis Outline.....	3
Chapter 2 Literature Review .....	4
2.1 Rubber and its Vulcanization .....	4
2.2 Scrap Rubber and Devulcanized Rubber .....	8
2.2.1 Scrap rubber.....	8
2.2.2 Devulcanized rubber .....	10
2.3 Differential Scanning Calorimetry (DSC).....	16
2.4 Models.....	19
2.5 Summary .....	26
Chapter 3 EXPERIMENTAL .....	28
3.1 Materials.....	28
3.2 Design of Experiments .....	29
3.3 Methods.....	30
3.3.1 Mixing: Batch Mixer .....	30
3.3.2 Characterization via DSC .....	31
Chapter 4 Kinetic Models .....	33
4.1 Calculation of Activation Energy .....	34
4.1.1 Arrhenius Model .....	34
4.1.2 Kissinger Model <sup>[66, 67]</sup> .....	35
4.2 Kamal-Sourour Model <sup>[56, 57]</sup> .....	37

Chapter 5 Results and Discussion .....	40
5.1 Natural Rubber and Devulcanized Rubber Samples .....	40
5.1.1 DSC.....	40
5.1.2 Statistical Analysis.....	46
5.1.3 Model Fitting .....	54
5.2 Master Batch Compound and Blends.....	58
5.2.1 DSC.....	58
5.2.2 Model Fitting .....	59
Chapter 6 Conclusions and Recommendations .....	67
Appendix A.....	70
Bibliography .....	75

## List of Figures

Figure 2.1: Network Formation <sup>[7]</sup> .....	4
Figure 2.2: Vulcanizate properties as a function of the extent of vulcanization <sup>[7]</sup> .....	5
Figure 2.3: Structural features of vulcanization network <sup>[6]</sup> .....	7
Figure 2.4: U.S. Scrap Tire Trends 2005-2011 <sup>[12]</sup> .....	9
Figure 2.5: U.S. Scrap Tire Disposition 2011 <sup>[12]</sup> .....	9
Figure 2.6: Difference in molecular structure of virgin, vulcanized and devulcanized rubber <sup>[14]</sup> .....	10
Figure 2.7: Breakage of crosslink points in high shear flow: (a) model for the chain; (b) deformation of network chain <sup>[27, 28]</sup> .....	13
Figure 2.8: Sampling position of devulcanized rubber <sup>[31]</sup> .....	14
Figure 2.9: Stabilization of sulphur by reaction with hydrogen atoms <sup>[32]</sup> .....	15
Figure 2.10: Power compensation DSC <sup>[47]</sup> .....	17
Figure 2.11: Heat Flux DSC <sup>[47]</sup> .....	18
Figure 2.12: DSC profile, showing exothermic heat flow with temperature <sup>[48]</sup> .....	19
Figure 3.1: Batch mixer used for mixing. ....	30
Figure 3.2: DSC thermogram for NR sample B at different scan rates. ....	32
Figure 4.1: Kissinger Model for NR sample B for activation energy calculation .....	36
Figure 4.2: Schematic of steps followed for model fitting .....	39
Figure 5.1: Graphical representation of the heat of reaction data for NR samples .....	42
Figure 5.2: Graphical representation of the heat of reaction data for DR samples .....	42
Figure 5.3: DSC curve for NR Sample B at different scan rates .....	43
Figure 5.4: DSC curve for DR Sample B at different scan rates .....	43
Figure 5.5: Peak temperature of different NR samples at different scan rates .....	44
Figure 5.6: Peak temperature of different DR samples at different scan rates .....	44

Figure 5.7: Pareto chart for Scan rate 15°C/min. ....	47
Figure 5.8: Pareto chart for Scan rate 20°C/min. ....	48
Figure 5.9: Pareto chart for Scan rate 20°C/min. ....	49
Figure 5.10: Pareto chart for Scan rate 25°C/min. ....	50
Figure 5.11: Predicted values versus observed values. ....	52
Figure 5.12: Effect of change in curative composition in total heat of reaction for NR and DR. ....	53
Figure 5.13: Fitted model vs. experimental data for NR sample B at 20°C/min. ....	55
Figure 5.14: Predicted data vs experimental data for NR sample B at 15°C/min. ....	56
Figure 5.15: Fitted model vs. experimental data for DR sample B at 15°C/min. ....	56
Figure 5.16: Predicted data vs experimental data for DR sample B at 20°C/min. ....	57
Figure 5.17: Fitted model vs experimental data for MB sample at 10°C/min. ....	60
Figure 5.18: Predicted data vs experimental data for MB sample at 40°C/min. ....	61
Figure 5.19: Fitted model vs Experimental data for MB/DR20 sample at 5°C/min. ....	62
Figure 5.20: Predicted data vs experimental data for MB/DR20 sample at 35°C/min. ....	63
Figure 5.21: Predicted data vs experimental data for MB/DR10 sample at 25°C/min. ....	64
Figure 5.22: Predicted data vs experimental data for MB/DR10 sample at 18°C/min. ....	64
Figure 5.23: Predicted data vs experimental data for MB/DR30 sample at 25°C/min. ....	65
Figure 5.24: Predicted data vs experimental data for MB/DR30 sample at 22.5°C/min. ....	66

## List of Tables

Table 2.1: CV, SEV and EV vulcanization systems <sup>[8]</sup> .....	7
Table 3.1: List of materials used. ....	28
Table 3.2: List of equipment used. ....	28
Table 3.3: Formulation for NR samples .....	29
Table 3.4: Formulation for DR samples .....	30
Table 3.5: Formulations for blends of master batch compound (Truck Tire Tread compound) and DR. ..	31
Table 5.1: Scans at Heating Rate of 20 °C/min for NR samples. ....	40
Table 5.2: Scans at Heating Rate of 20 °C/min for DR samples. ....	41
Table 5.3: ANOVA at a Scan rate 15°C/min for Natural Rubber Samples; $R^2=0.99624$ ; 2**(2-0) design .....	46
Table 5.4: ANOVA at a Scan rate 20°C/min for Natural Rubber Samples; $R^2=0.98023$ ; 2**(2-0) design. .....	47
Table 5.5: ANOVA at a Scan rate 20°C/min for Devulcanized Rubber Samples; $R^2=0.97918$ ; 2**(2-0) design.....	48
Table 5.6: ANOVA at a Scan rate 25°C/min for Devulcanized Rubber Samples; $R^2=0.96175$ ; 2**(2-0) design.....	49
Table 5.7: Significant Variables at different scan rates. ....	51
Table 5.8: Regression Coefficients at 15°C/min for Natural Rubber Samples. ....	51
Table 5.9: Estimated constants for NR sample B. ....	54
Table 5.10: Estimated constants for DR sample B. ....	55
Table 5.11: $T_{peak}$ and total heat of reaction for the MB compound. ....	58
Table 5.12: $T_{peak}$ and heat of reaction for MB/DR20 blends. ....	58
Table 5.13: $T_{peak}$ and heat of reaction for MB/DR10 blends. ....	59

Table 5.14: T <sub>peak</sub> and heat of reaction for MB/DR30 blends. ....	59
Table 5.15: Estimated constants for MB. ....	60
Table 5.16: Estimated constants for MB/DR20. ....	61
Table 5.17: Estimated constants for MB/DR10. ....	63
Table 5.18: Estimated constants for MB/DR30 ....	65
Table A.1: Scans at Heating Rate 5 °C/min.....	70
Table A.2: Scans at Heating Rate 10 °C/min.....	70
Table A.3: Scans at Heating Rate 15 °C/min. ....	71
Table A.4: Scans at Heating Rate 15 °C/min.....	71
Table A.5: Scans at Heating Rate 25 °C/min.....	71
Table A.6: Estimated constants for NR Sample A. ....	72
Table A.7: Estimated constants for NR Sample C. ....	72
Table A.8: Estimated constants for NR Sample D. ....	72
Table A.9: Estimated constants for NR Sample E. ....	73
Table A.10: Estimated constants for DR Sample A. ....	73
Table A.11: Estimated constants for DR Sample C. ....	73
Table A.12: Estimated constants for DR Sample D. ....	74
Table A.13: Estimated constants for DR Sample E.....	74

## List of Abbreviations and Symbols

°C	Degrees Celsius
CBS	N-Cyclohexyl-2-benzothiazole sulfenamide
C-C	Carbon Carbon Bonds
C-S	Carbon-Sulphur Bonds
DMA	Dynamic mechanical analysis
DR	Devulcanized rubber
DSC	Differential Scanning Calorimetry
DTA	Differential thermal analysis
Eqn.	Equation
EPDM	Ethylene propylene diene monomer
FTIR	Fourier transform infrared Spectroscopy
gm	Gram
HAF	High furnace carbonblack
MDR	Moving Die Rheometer
NR	Natural Rubber
ODR	Oscillating Disc Rheometer
scCO <sub>2</sub>	Supercritical carbondioxide
St.A	Stearic acid
TGA	Thermo Gravimetric Analysis
TBBS	N-tert-butyl-2-benzothiazyl Sulfenamide

# Chapter 1

## Introduction

### 1.1 Motivation

Commercial use of rubber boomed after Charles Goodyear discovered the vulcanization technique in 1839, as raw rubber did not have enough strength and dimensional stability to be used for rubber products. Vulcanization (curing) is a chemical process in which cross links are formed between individual polymer chains and it can improve the properties of rubber products. It changes the rubber into a thermoset polymer which means it cannot be reprocessed simply by application of heat or separated into their chemical components.

Vulcanization improved the properties of rubber products, but at the same time it made the disposal/recycling of rubber products almost impossible. Since the scrap generated from rubber products is immune to biological degradation, simply dumping it is not a solution. Land filling and stockpiling were the most common ways of tire disposal, but the discarded tires in landfills tend to rise up to the surface. Land filling also leads to wastage of land and land pollution. Stockpiled tires act as a breeding ground for mosquitoes and rodents, posing health hazards. Also, large piles of tires often pose fire hazards. Thus, proper steps must be taken while dealing with these scrap material to prevent environmental problems.

Among all the rubber products in use today (like footwear, seals, gaskets, tiles, hose, conveyor belts, etc.), tires occupy a large percentage of the rubber product market. With the growth of the automotive industry, uses of tire are increasing day by day, which is resulting in an increased scrap tires generation. As it is difficult to dispose these scrap tires, it is important to reduce, reuse and recycle the scrap. The presence of the chemical cross links between the polymer chains make it essential to modify the scrap rubber to be able to reprocess and reuse them. The process in which

the scrap tire rubber or vulcanized rubber is converted, using mechanical energy, thermal energy and chemicals, into a processable and vulcanizable material is called reclamation (or devulcanization) and the rubber obtained is called reclaimed rubber (or devulcanized rubber) <sup>[1]</sup>. Different type of reclamation methods are being developed to present date.

Reusing of scrap rubber not only helps in protecting the environment but also helps us reclaim a low cost usable resource. Cost reduction is possible if a certain amount of virgin rubber can be replaced with devulcanized rubber (DR). Also, due to the intense treatment given to the rubber in the reclamation process, it can be expected to break down more quickly than virgin rubber, which means a reduction in mixing cycles and thus more savings <sup>[2]</sup>.

After the scrap rubber is modified the next important step is to put it into application. The properties of such material remain inferior compared to a virgin rubber so the method of reclamation chosen must produce reclaim rubber of very high quality. Also, the DR obtained may not behave in the same manner compared to that of virgin rubber during the vulcanization process. So it would be helpful if a proper model could be obtained in order to characterize and optimize the vulcanization properties of DR with respect to the vulcanizing agents added.

## **1.2 Research Objectives**

The main objective of this study is to characterize the vulcanization reaction of DR by a kinetic model using differential scanning calorimetry (DSC). This will help in predicting the kinetics of vulcanization with change in temperature and amount of curatives added. Also, it will help to obtain a better understanding of the curing behavior and properties of DR. It will further assist in minimizing the time required for choosing the appropriate cure system for compounds involving DR. The main challenge is to use the data obtained from DSC and fitting the model to the data that can best describe the vulcanization reaction of DR.

One of the objectives is also to study the curing behavior of virgin rubber and DR to have a comparison between both. To further analyze the cure kinetics of DR, a study of the curing behavior of blends of virgin rubber with 10, 20 and 30% of DR was done.

### **1.3 Thesis Outline**

The thesis is divided into six chapters. Chapter 1 introduces the importance and challenges of the project. Chapter 2 provides a literature review and throws some light on the basic theory related to the research and glimpse of the research work done so far in similar areas. Chapter 3 discusses about the experiments carried out along with the materials, equipment and characterization method used. Chapter 4 describes the models used in this project to characterize the vulcanization reaction. Chapter 5 summarizes the results obtained from all the experiments and the estimated kinetic parameters. Chapter 6 provides the concluding remarks considering the results obtained.

## Chapter 2

### Literature Review

#### 2.1 Rubber and its Vulcanization

“Caoutchouc”, meaning ‘tears of the wood’, was the term used for natural rubber by natives of South America. Columbus, during his voyage in 1493-6, was the first European to see rubber in the form of play balls used by natives of Haiti. In 1770, Joseph Priestly found that this solid mass can rub off pencil marks from paper and, hence, he termed it as ‘rubber’<sup>[3-4]</sup>. This material was used in some applications like footwear or applications where rubber was supported by fabric but raw rubber was relatively weak and it melted and developed an offensive smell during the summer. It was only after 1840, when Charles Goodyear discovered the vulcanization process (heating of raw natural rubber with sulphur as cross linking agent), that the commercial use of rubber flourished<sup>[5-7]</sup>.

Vulcanization is a chemical process in which the sticky rubber is heated in presence of a cross linking agent which modifies it into a non-sticky, more durable product by forming bonds between individual polymer chains (Figure 2.1). Improvements due to curing in the rubber product properties, like tensile strength, modulus, tear strength, etc. are seen in Figure. 2.2 as a function of crosslink density.

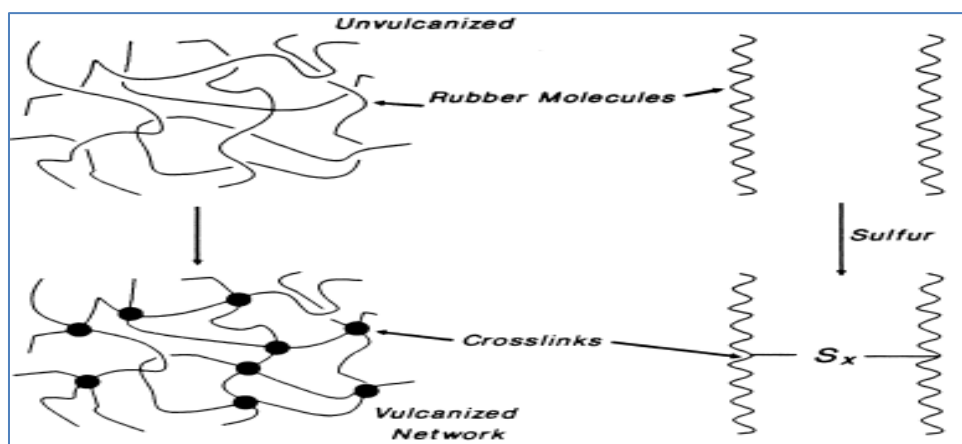


Figure 2.1: Network Formation<sup>[7]</sup>.

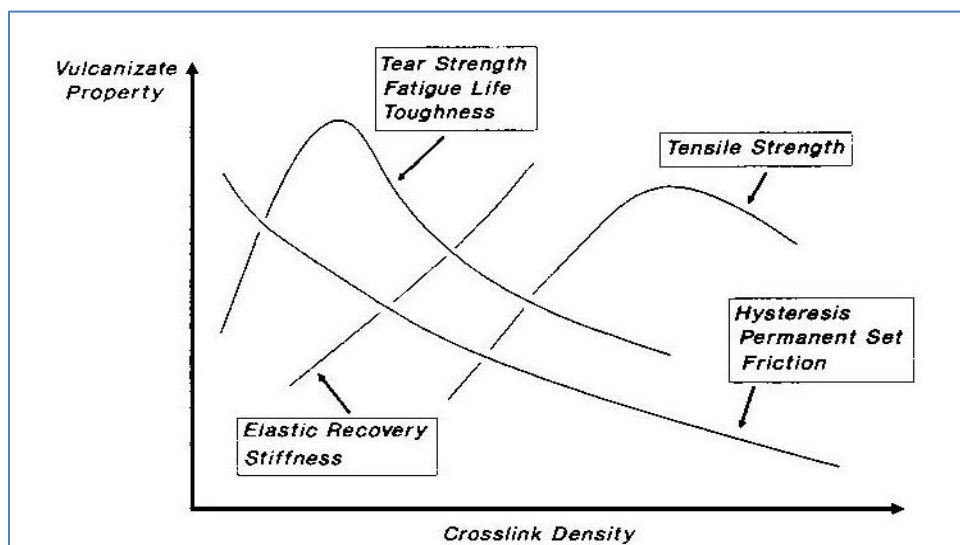


Figure 2.2: Vulcanizate properties as a function of the extent of vulcanization [7].

The vulcanization process developed by Goodyear has been gradually improved over time. In addition to natural rubber (NR) many synthetic rubbers have been developed. Also, with cross linking agents other materials (like accelerators and activators) were introduced to the vulcanization system to decrease the vulcanization time and improve the vulcanizate properties [6-8].

Generally, sulphur is in general the most common vulcanizing agent used, which requires the presence of unsaturation to form cross links. Varieties of accelerators (like 2-mercaptobenzothiazole, 2,2'-dithiobenzothiazole, N-cyclohexylbenzothiazole-2-sulfenamide, etc.) are also used along with sulphur. These chemicals increase the rate of vulcanization, thus reducing the overall time for the reaction. Activators are also used with sulfur and accelerators, and they assist to increase the rate of reaction by forming chemical complexes with accelerators.

The chemistry of sulphur vulcanization is very complex and the unravelling of the process took a long time but even today there is paucity of knowledge pertaining to the exact chemistry involved in the vulcanization process. The detailed chemistry of vulcanization is not discussed here.

- **Vulcanization using sulphur as a cross linking agent**

Many studies have been done on vulcanization of rubber using sulphur as a curing agent. Coran<sup>[9]</sup> provided a kinetic scheme for sulphur vulcanization with and without accelerators. From the scheme provided by Coran<sup>[9]</sup> and Blow<sup>[6]</sup>, steps involved in accelerated sulphur vulcanization can be summarized in brief as follows:

Typically a recipe for vulcanization systems consists of elastomer, sulphur, accelerator, and zinc oxide and fatty acid as activators.

- Zinc oxide and fatty acids form a salt that can form complexes with accelerator and reaction products from accelerator and sulphur which assist in the vulcanization reaction.
- Sulphur reacts with the zinc salt of the accelerator to give monomeric polysulfides of structure Ac-S<sub>x</sub>-Ac, where Ac is a group derived from the accelerator.
- The monomeric polysulfide reacts with the rubber hydrocarbon to form polymeric polysulfides, i.e. rubber-S<sub>x</sub>-Ac. It may then react to give rubber bound intermediates and a perthio accelerator group.
- Finally, the rubber polysulfides react, either directly or by forming intermediates to give cross links.

As crosslink in the vulcanization network, sulphur is seen to combine in a number of ways (Figure 2.3); like: **a.** Monosulfide, **b.** Disulfide, **c.** Polysulfide, **d.** Pendent sulfide, **e.** Cyclic monosulfide, **f.** Cyclic disulfide <sup>[6]</sup>. The degree of polysulfidity of cross links declines with increased heating <sup>[9]</sup>.

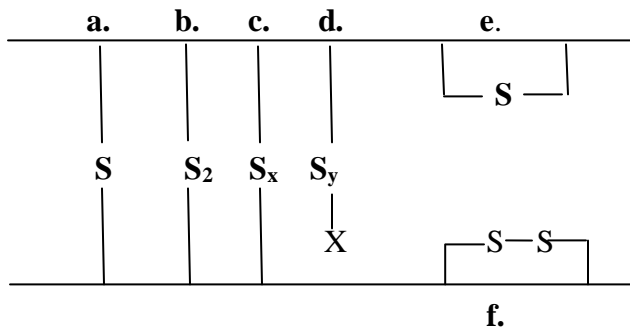


**Figure 2.3: Structural features of vulcanization network <sup>[6]</sup>.**

Depending on the sulfur to accelerator ratio, three special types of cure systems have been developed over the years: conventional vulcanization (CV), semi-efficient vulcanization (SEV) and efficient vulcanization systems (EV). Typical recipes are listed in Table 2.1.

**Table 2.1: CV, SEV and EV vulcanization systems <sup>[8]</sup>.**

Type	Sulfur (S, phr)	Accelerator (A, phr)	A/S ratio
CV	2.0-3.5	1.2-0.4	0.1-0.6
SEV	1.0-1.7	2.4-1.2	0.7-2.5
EV	0.4-0.8	5.0-2.0	2.5-12

## 2.2 Scrap Rubber and Devulcanized Rubber

### 2.2.1 Scrap rubber

Recycling of scrap rubber is not a new area of research. Increasing demand and price of raw NR led to recycling efforts of scrap rubber. Charles Goodyear himself has a patent on one of the reclaiming techniques <sup>[2]</sup>. Over time and advancement in automotive industry, scrap tire management has become a growing problem. Over 240 million scrap tires are generated each year in the United States. In addition, 2 billion scrap tires have accumulated in stockpiles or uncontrolled dumping <sup>[10]</sup>. Some facets of this problem are listed below:

- a. Tires act as a breeding ground for mosquitoes and rodents posing risk for many diseases.
- b. Stock piles of tires pose fire hazards. Once a fire starts in a stockpile of tires it not only gives out harmful gases but is also difficult to extinguish.
- c. Land filling of tires can result in wastage of land and also cause land pollution, as various compounding ingredients in the tire can leach out from the bulk to the surface.
- d. Awareness of this problem has led us to find alternative paths to deal with the scrap tires. Substantial opportunities for recycling and reusing of waste tires are developed which include tire retreading, asphalt pavement containing recycled rubber, tire derived fuel (TDF), etc <sup>[10-13]</sup>.

According to U.S. Environmental Protection Agency, markets now exist for around 80% of scrap tires from 17% in 1990. It is expected that in the future most of the scrap rubber will be recycled in the form of reclaim because of the increase in environmental awareness <sup>[13]</sup>.

A Rubber Manufacturers Association's (RMA) 2011 US Scrap tire Market summary (Figure 2.4) shows that the amount of scrap tires utilized in 2011 decreased around 3-7% compared to 2007 and 2009 but percentage of scrap tire utilization still remains above 80%.

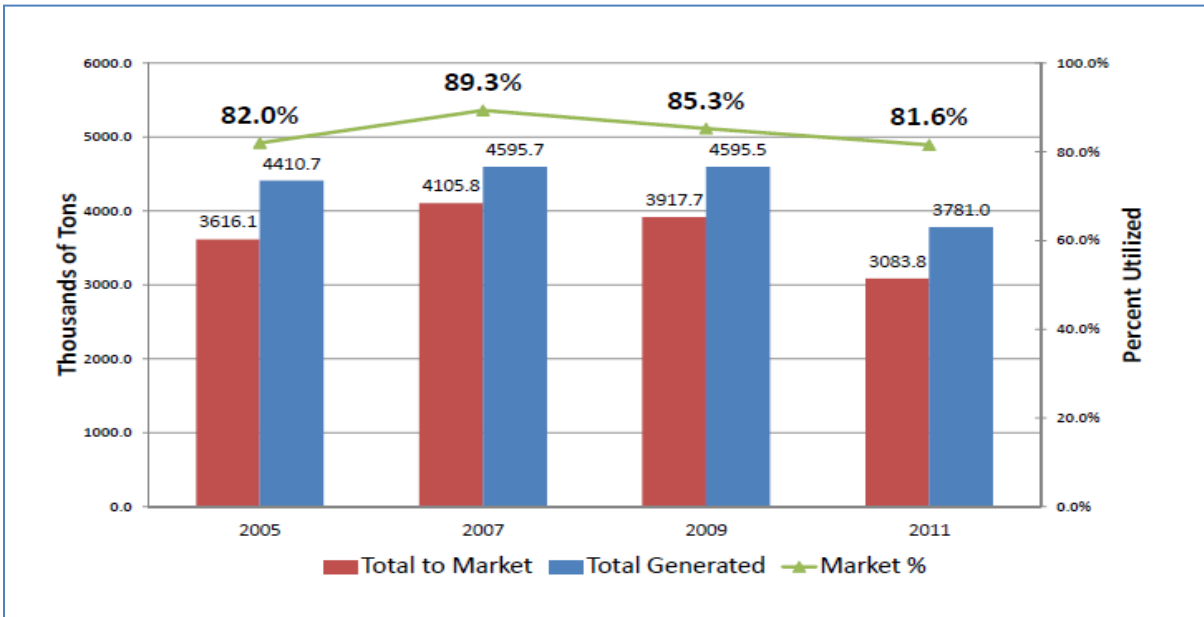


**Figure 2.4: U.S. Scrap Tire Trends 2005-2011** <sup>[12]</sup>.

Figure 2.5 shows that the major amount of scrap tires was consumed as TDF followed by ground rubber and land disposal. The TDF market actually decreased from 52.8% in 2007 to 37.7% in 2011 and an increase in ground rubber market from 16.8% in 2007 to 24.5% in 2011 was observed <sup>[11, 12]</sup>.

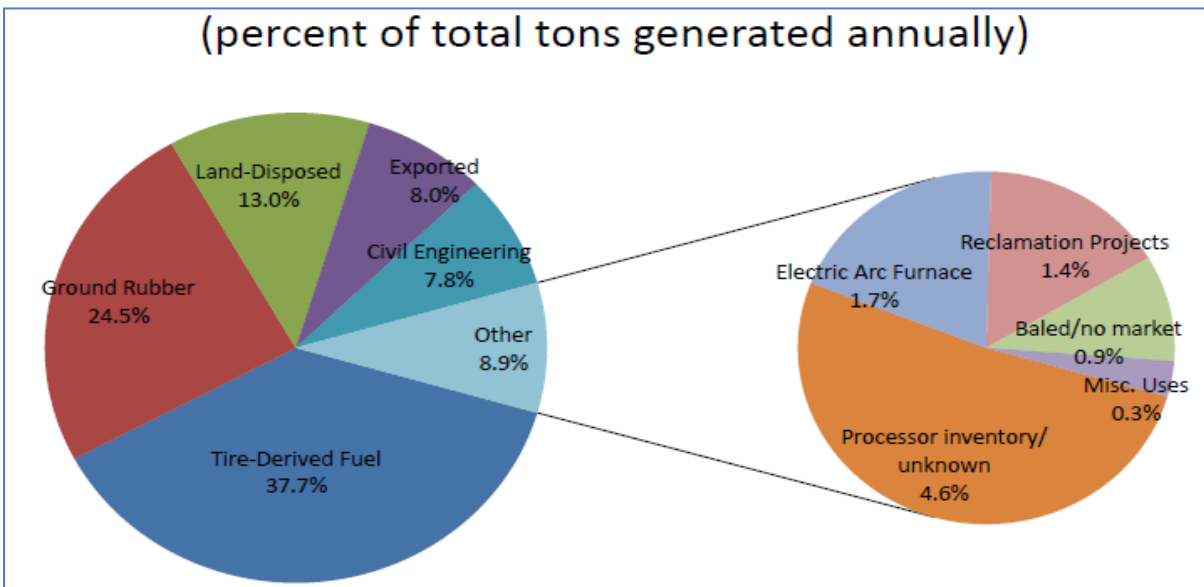


**Figure 2.5: U.S. Scrap Tire Disposition 2011** <sup>[12]</sup>.

### 2.2.2 Devulcanized rubber

The process in which the cross links in the vulcanized rubber are partially or totally cleaved is termed as devulcanization. It is preferred that during devulcanization main chain scission is avoided to have better properties. Once the vulcanized rubber is devulcanized it can be processed and revulcanized like a virgin rubber. Figure 2.6 shows the molecular structure of virgin rubber, vulcanized rubber and devulcanized rubber.

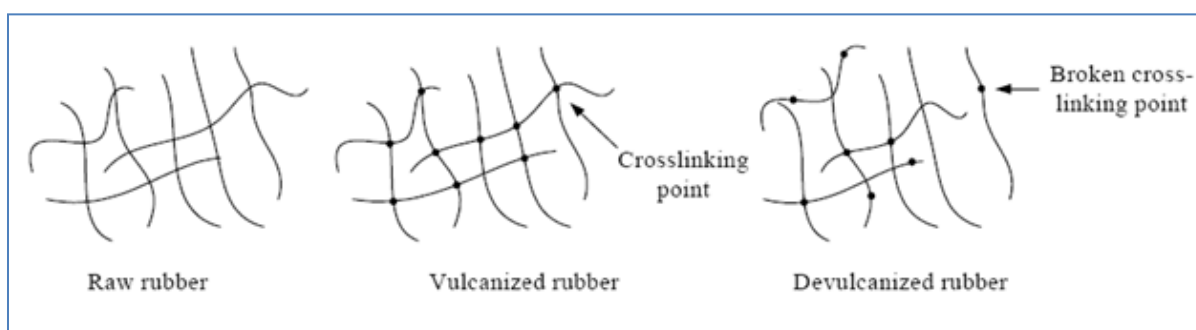


**Figure 2.6: Difference in molecular structure of virgin, vulcanized and devulcanized rubber** <sup>[14]</sup>.

Different methods for devulcanization have been developed and some of them are briefly described below.

- a. **Thermo-Chemical methods:** In this process chemicals are added along with thermal energy to break the three dimensional cross linked networks.

➤ **Digester Process**

A digester is essentially a steam-jacketed, agitator-equipped autoclave mounted either horizontally or vertically. In this process ground rubber, water, and reclaiming and defibering agents are dumped into the digester and the cook cycle is started. Steam, generally within the range of 150 to 250 psi, is injected for the digestion period that may be 5 to 24 hours. The rubber becomes devulcanized and the fibre becomes hydrolyzed during this time. After digestion the charge is blown down, washed and conveyed to a dryer <sup>[2, 6]</sup>.

➤ **Heater or Pan Process**

The ground rubber, (fabric free) is mixed with reclaiming agents in an open ribbon mixer then placed into steam vulcanizers. Live steam at pressure of 100 to 250 psi with cycle times 5 to 12 hours is given. The main consideration is to allow even penetration of heat in the mass of rubber <sup>[2, 6]</sup>.

➤ **Engelke Process**

In this process the vulcanized scrap rubber containing fabric is subjected to very high temperatures for a period of around 10-20 min in small autoclaves. Any fabric that is present is completely carbonised in situ. The reclaimed rubber (or devulcanized rubber) is then strained and refined <sup>[6]</sup>.

**b. Thermo-Mechanical Methods:** To break the cross linked network, stresses are used along with thermal energy.

➤ **Mixing Mill**

This process is also called mechanical process. In this process crumb rubber is placed in an open two roll mixing mill and mixing is carried out at high temperature around 200 °C. A process developed by Maxwell <sup>[15]</sup> for reclaiming vulcanized rubber involves feeding particulate vulcanized rubber between a stator and a rotor having smooth opposing surfaces and thus providing an axial shear zone in which rubber is propelled. Another group reported the mechanical reclaiming process of natural rubber (NR) by milling vulcanized sheet on a two roll mixing mill at about 80 °C <sup>[13]</sup>.

➤ **Microwave method**

Microwave technology applies the heat very quickly and uniformly on the waste rubber. It has the advantage of giving controlled dose of energy at specific frequency to devulcanize a sulphur vulcanized elastomer, containing polar groups or components, to a state in which it could be compounded and revulcanized to useful products <sup>[1, 13, 18]</sup>. Tyler and Cerny <sup>[16]</sup> claimed their process as a method of pollution-controlled reclaiming of sulphur vulcanized elastomers. Also, the devulcanized material is not degraded when recycled, which normally takes place in usual commercial methods <sup>[17]</sup>.

➤ **Ultrasonic Method**

Though ultrasound is seen to be used to vulcanize rubber rather than devulcanization, many studies have been done where devulcanization using ultrasonic energy is achieved <sup>[1, 19-22]</sup>. A process in which rubber articles immersed in a liquid is exposed to ultrasonic energy resulting in disintegration of the bulk rubber and finally the rubber dissolves into the liquid. This is the first work done with ultrasonic energy patented by Pelofsky in 1973<sup>[19]</sup>. Also rubber devulcanization by using ultrasound is discussed in Okuda and Hatano <sup>[1, 20]</sup>, the process claimed to break carbon-sulphur bonds and sulphur-sulphur bonds and not carbon-carbon bonds thus revulcanized DR were found to be very similar to original vulcanizates. Isayev and co-workers <sup>[1, 20-24]</sup> have carried out several studies using ultrasonic energy for devulcanization using a coaxial ultrasonic devulcanization reactor. They also devulcanized EPDM using a continuous ultrasonic grooved barrel reactor.

➤ **Twin Screw Extrusion**

Devulcanization using twin screw extruders is one of the relatively new methods of devulcanization. During this process, shear and elongational stresses along with high temperature are used for breaking the three dimensional crosslink networks resulting in a processable and revulcanizable

product. But the stress and heat used can also break down the main chain of polymer resulting in poor properties. So one of the main considerations while devulcanizing should be to cleave the crosslink bonds selectively thus breaking the carbon-sulphur bonds or sulphur-sulphur bonds rather than carbon-carbon bonds. It was observed that processing parameters and equipment characteristics play an important role in selective cleaving of crosslink bonds <sup>[25, 26]</sup>. The difference in bond energies (Figure 2.7a) between carbon-carbon(C-C), carbon-sulphur(C-S) and sulphur-sulphur(S-S) bonds is very small and hence under pressure and heat unselective cleavage may occur. On other hand, if we consider the elastic constants for these bonds, S-S bonds can be estimated to be about 1/30<sup>th</sup> of the one for the C-C bonds (Figure 2.7b). Under high shear stress the bonds having lower value (S-S) of elastic constant may become more extended compared to the one having higher value (C-C), thus favouring cleavage of S-S bonds <sup>[27, 28]</sup>.

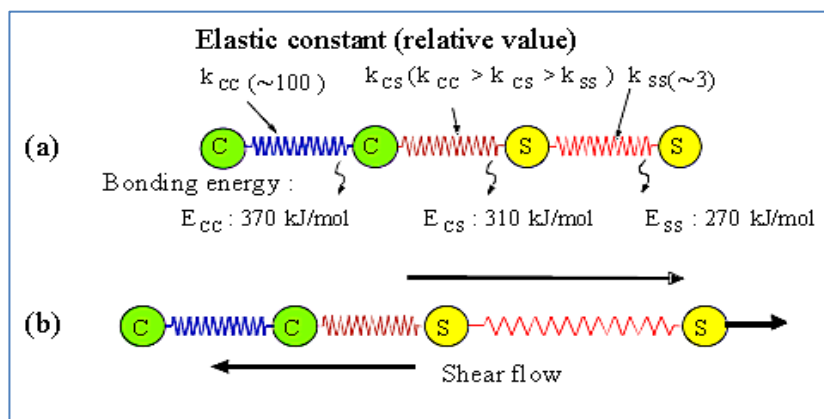


**Figure 2.7: Breakage of crosslink points in high shear flow: (a) model for the chain; (b) deformation of network chain <sup>[27, 28]</sup>.**

The use of a co-rotating twin screw extruder for continuous devulcanization of EPDM (ethylene propylene diene monomer) using shear flow stage reaction technology has been reported by Mouri et al <sup>[29-32]</sup>. The process involves using a shear flow stage reactor, with selective shearing of cross links of the rubber under proper conditions (screw shape, screw speed, pressure and treatment

temperature) without the use of devulcanizing agent. They investigated the effect of various processing parameters on devulcanized rubber properties and concluded that DR has almost same curing characteristics, formability and mechanical properties as virgin material <sup>[30]</sup>. They also studied devulcanization process of rubber inside the reactor by removing the screw during devulcanization and sampling the material at different points (Figure 2.8). It was seen that the gel fraction and the effective network chain density decreases with increasing screw speed <sup>[31]</sup>.

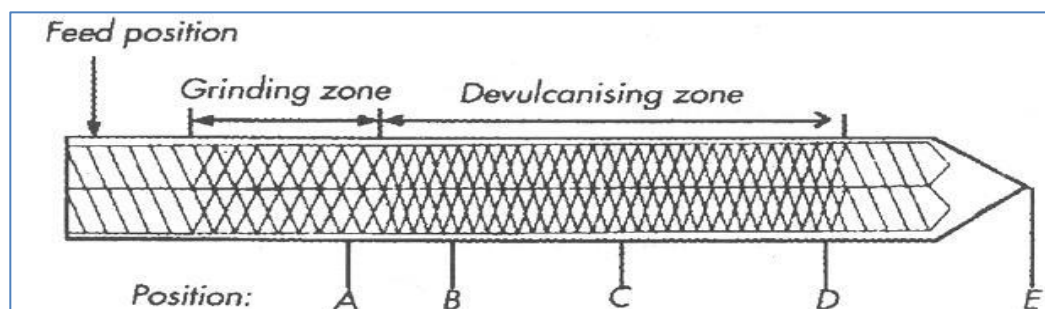


**Figure 2.8: Sampling position of devulcanized rubber <sup>[31]</sup>.**

Another study <sup>[32]</sup> analysed the changes in the network structure during devulcanization treatment, breakdown of sulphur cross links and devulcanization mechanism. It was found that at the beginning of the reaction the polysulphide and disulphide bonds were converted by heat to monosulphide bonds. These monosulphide bonds were thought to be broken down later by application of shear force. The sulphur atoms in the broken sulphur cross links are seen to react with hydrogen atoms <sup>[32]</sup>.

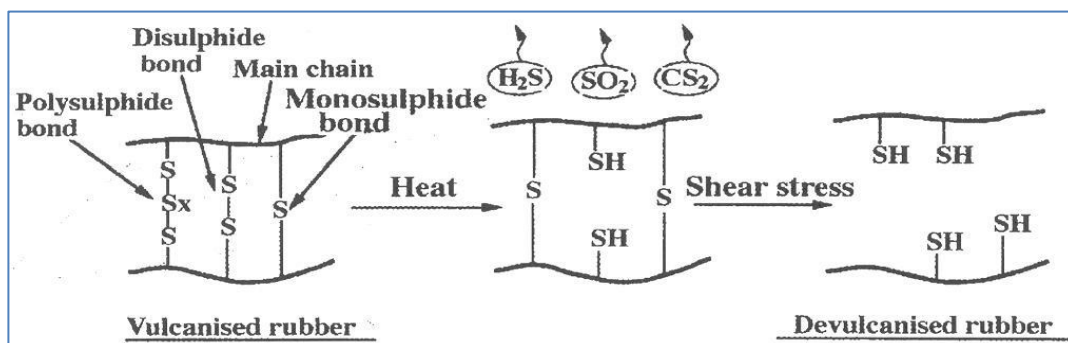


**Figure 2.9: Stabilization of sulphur by reaction with hydrogen atoms <sup>[32]</sup>.**

The same technology was further developed by Fukumori et al <sup>[27, 28]</sup> in which they used a modular screw type reactor (twin screw extruder). They also studied temporal changes in the rubber matrix during the dynamic devulcanization process by removing the screw from the barrel and sampling the materials. Various parameters like Mooney viscosity, the fractions of gel and sol components, effective network chain density, etc. were studied. The devulcanized EPDM was compounded and cross linked using the conventional recipe and they found that the properties of the product from devulcanized EPDM was almost equal to those of new rubber.

Maridas and Gupta <sup>[33-35]</sup> have developed a devulcanization process which uses counter rotating twin screw extruder for the process. They used models (four parameter logistic model) and statistical tools (central composite rotatable design) to study and optimize the devulcanization process. Also, the effects of carbon black and sulphur to accelerator ratios on the properties of products using devulcanized rubber were studied. It was concluded that optimum properties were achieved with the use of 15phr HAF (high abrasion furnace) carbon black and 1.5/0.75 ratio of sulphur/accelerator. Sutanto et al. <sup>[36]</sup> and, Karrabi and Ghasemi et al. <sup>[37, 38]</sup> have also studied devulcanization reaction using experimental designs.

Research involving the use of supercritical carbon dioxide (scCO<sub>2</sub>) with devulcanizing agents (diphenyl disulphide, etc.) for devulcanization in a pressurized autoclave was developed by Kojima et al. and a

number of papers were published based on their work <sup>[39-41]</sup>. They used scCO<sub>2</sub> to improve the diffusion of devulcanizing agents. It was concluded that the use of scCO<sub>2</sub> resulted in enhanced rate of devulcanization. Another method for devulcanization involving scCO<sub>2</sub> was developed in our lab by Tzoganakis and was patented <sup>[42]</sup>. This process of devulcanization in twin screw extruder uses mechanical elongation and shear forces in presence of scCO<sub>2</sub>. The purpose of injecting scCO<sub>2</sub> in the extruder is to facilitate the extrusion process and this is achieved by penetration of scCO<sub>2</sub> in the rubber crumb particles which causes them to swell. Swelling results in exerting more stress on less elastic cross links(C-S and S-S bonds), thus making them more susceptible for cleavage. Studies were carried out to investigate the effect of processing parameters and properties of devulcanized rubber obtained using this method by Tzoganakis and Zhang <sup>[43]</sup>. This work was further expanded by Meysami <sup>[26, 44-46]</sup> to scale up the devulcanization process in order to achieve a higher throughput of devulcanized rubber. Also, studies on the curing behaviour and mechanical properties of different compounds consisting blends of virgin and devulcanized rubber along with effect of process parameters on properties were evaluated. It was concluded that feeding rate and screw speed are the key parameters to control processability. Also, with the increase in feed rate, sol fraction decreases and crosslink density increases. The DR obtained can be revulcanized by adding curing agents to get a product with reasonable physical and mechanical properties.

### **2.3 Differential Scanning Calorimetry (DSC)**

DSC is widely used to study the vulcanization reaction of rubbers. It is a thermal analysis method which studies properties of material that change with temperature. Different methods of thermal analysis used to study the thermo-physical properties of material are DSC, differential thermal analysis (DTA), thermo gravimetric analysis (TGA), etc. DSC can be said to be an experimental technique used for measuring the energy necessary to establish a nearly zero temperature difference between a sample (S)

and reference (R) material, while both are subjected to a controlled temperature program. DSC can monitor phase transitions and chemical reactions as a function of temperature <sup>[47- 49]</sup>.

There are two most common types of DSC:

- **Power Compensation DSC:** In this case the specimen and reference temperatures are controlled independently by separate ovens. The power input is varied in order to maintain a zero temperature difference between the two (Figure 2.10).

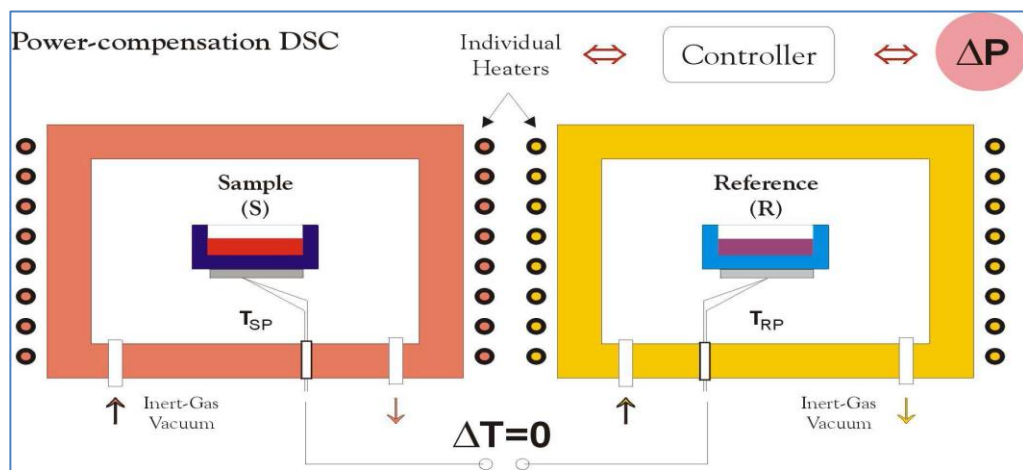


**Figure 2.10: Power compensation DSC <sup>[47]</sup>.**

- **Heat Flux DSC:** In this case both sample and reference (usually an empty pan) are in same furnace with a metallic block having a high thermal conductivity which ensures good heat flow between S and R. Due to the change in enthalpy or heat capacity of sample, temperature difference between S and R is observed, which is recorded and related to enthalpy change in the specimen (Figure 2.11).

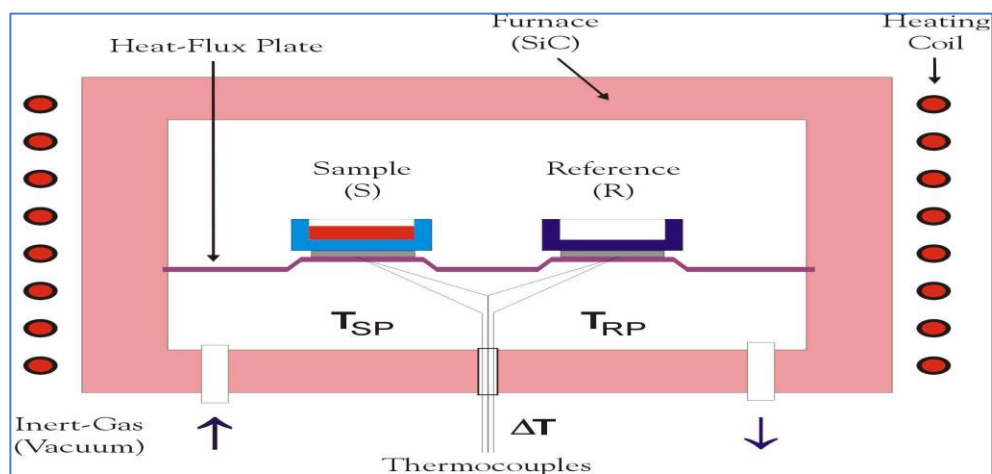


**Figure 2.11: Heat Flux DSC** <sup>[47]</sup>.

DSC experiments are either performed isothermally or with a change in temperature at a constant rate. In the case of isothermal experiments, DSC signals are plotted against time for a constant temperature. For dynamic tests, the DSC signals are plotted against either time or temperature. As the scanning of a particular sample continues, the computer program attached to DSC records the temperature, heating rate and the difference in heat flow between the reference pan and the sample, i.e. the heat flow for the sample. A plot can be obtained from the data recorded as shown in Figure 2.12. The slope of the curve is the rate of change heat capacity. Different reactions yield different types of DSC curves. For example, in Figure 2.12 it can be seen that in the case of cross-linking which involves release of heat (exothermic reaction), the peak is upwards compared to a melting process which takes in heat (endothermic reaction).

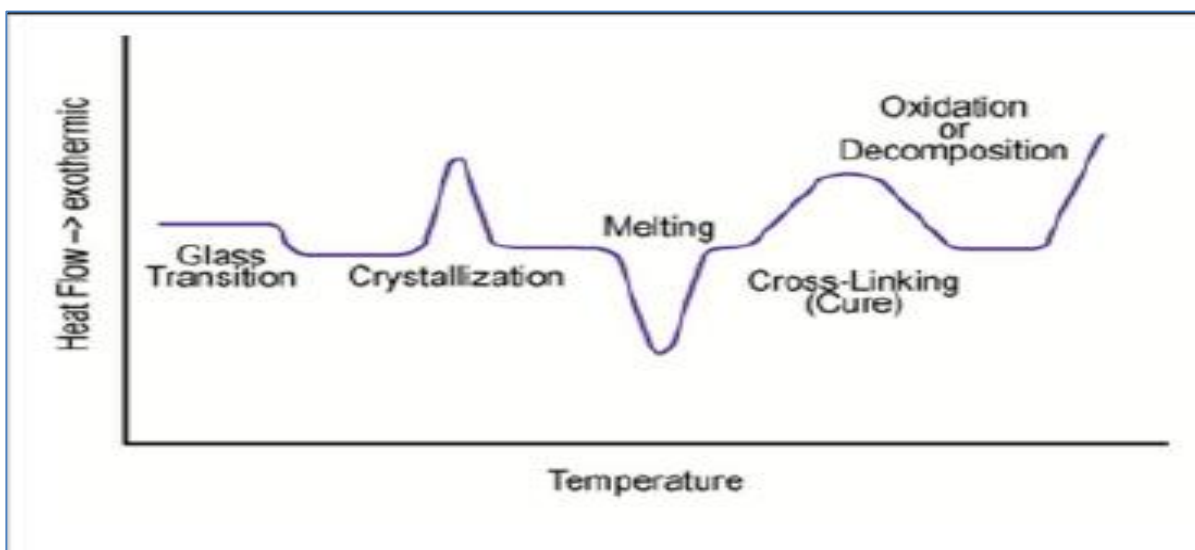


**Figure 2.12: DSC profile, showing exothermic heat flow with temperature <sup>[48]</sup>.**

For characterization of the vulcanization of rubbers, DSC can be used either as isothermal mode or non-isothermal (dynamic) mode or both. In the case of isothermal scans it is challenging to reach the desired temperature as fast as possible, moreover due to the fast reaction rate one may miss the important part of reaction before the desired temperature is reached. Also, as the isothermal technique can be used to determine kinetic model constants at one temperature, finding the temperature dependence of the kinetic parameters requires additional experimental work and parameter estimation.

## 2.4 Models

After the scrap rubber is devulcanized it is reprocessible, but to make it into a usable product we need to vulcanize it again. Vulcanization of the DR has been studied by many researchers <sup>[18, 23, 43, 44 and 46]</sup>. It was observed that some changes in the chemical structure of the polymer occur resulting in differences in the curing characteristics compared to the vulcanized rubber.

Isayev et al. <sup>[23]</sup> investigated curing behaviour of compounds based on virgin rubber and ultrasonically devulcanized SBR (styrene butadiene rubber). Both the compounds were vulcanized using sulphur and

CBS (accelerator). The curing behaviour was investigated using both oscillating-disc cure meter (ODR) and differential scanning calorimetry (DSC) apparatus and it was observed that there are strongly pronounced differences between the curing behaviour of virgin and devulcanized rubber. The induction period that is generally seen in cure curves for virgin rubber was much shorter or absent in the case of devulcanized rubber. Also, the DSC curve for DR was seen to have double peaks indicating that vulcanization of DR proceeds in two steps whereas curing of virgin rubber is characterized by a single peak. Some differences observed in the curing behaviour of DR were thought to be the effect of an interaction between rubber molecules chemically modified in the devulcaniation process and non-modified molecules which results in cross linking. Work done by Tzoganakis et al. <sup>[43]</sup> on devulcanized rubber showed that FTIR spectroscopy analysis indicated significant changes occurred in the chemical structure of recycled rubber crumb. This change in the chemical structure of DR can have an effect on the vulcanization reaction. Also, a study done by Meysami <sup>[44, 46]</sup> showed that although the DR can be revulcanized by adding curing agents to get reasonable properties, the curing behaviour of compound containing 100% DR is different compared to 100% virgin rubber compound.

Another group <sup>[18]</sup> studied the chemical modification which occurs in SBR after microwave devulcanization. They showed that microwave treatment causes cleavage of mainly polysulfidic cross links and decomposition of chemical groups having sulphur attached to the chemical structure of SBR leaving mainly monosulfidic bonds. FTIR spectroscopy analysis showed a decrease in carbon-carbon double (C=C) bonds which are important for sulphur vulcanization as sulphur creates cross links via these structures. So a decrease in C=C can affect the revulcanization and final properties of the DR.

From the studies conducted to investigate the curing behaviour of DR it can be said that the curing characteristics of DR differ from that of a virgin rubber. So it would be helpful if a model that can predict the vulcanization reaction is available. This will help in having a clear understanding of the curing behaviour of DR and also decrease the time required for choosing an appropriate curing system for DR.

Simulation of vulcanization reaction of different rubber compounds using a kinetic model is not so new topic. However, modelling the vulcanization reaction of DR is comparatively a new area of study. So far only a limited amount of data <sup>[50]</sup> on the attempts to model the kinetics of DR is available.

Cure kinetics of rubber depend on many factors. Some of the most important are composition of rubber compound, test temperature and the methods used to characterize the same. Several techniques have been used to characterize vulcanization reaction of different rubbers like DSC, MDR, ODR, FTIR, etc. All these methods determine the degree of cure with respect to time/temperature allowing us to understand the extent of cure with time for a specific compound <sup>[51]</sup>.

Different kinetic models have been developed so far; a list of models for thermosetting system is given by Halley and Mackay in one of their papers <sup>[52]</sup>. Generally, all these models fall into two categories: mechanistic and phenomenological or empirical models. The mechanistic models analyse vulcanization as a series of chemical reactions and model each of them. They are based on stoichiometric balances of reactants involved in each reaction to form mathematical relations between reaction rate with cure time and temperature. Thus, it involves detailed measurements of concentration of reactants, intermediates and product. Although these models can represent the kinetics of vulcanization better, the complexity of vulcanization reactions makes this approach essentially more difficult to apply. Phenomenological or empirical models on the other hand assume vulcanization as a whole process. These models do not provide a clear description of the vulcanization process/reactions and the chemistry behind it. The main features of such a model is that they are regression models that fit data assuming a particular functional form and they describe the rate of reaction as a function of reactant concentrations and rate constants. These models are simpler to compute and can be widely used to model vulcanization reactions.

Although modelling through the mechanistic approach is difficult, many researchers have used such models. Coran <sup>[9]</sup> gave a kinetic scheme for sulphur vulcanization of NR. Using this scheme Ding and

Leonov <sup>[53]</sup> proposed a model to simulate induction, curing and over cure periods. They used both cure meter (RPA 2000) and DSC to study rubber vulcanization and concluded that cure meter technique is more reliable than DSC. Due to more than one reaction (side reactions) occurring during vulcanization (multiexothermal reactions) the heat data from DSC do not have a simple correlation to the curing data from the cure meter. Their model prediction showed a good agreement with the isothermal cure meter experimental data over the studied temperature range. Further Ding et al. modified Coran's model to develop a model that includes side reactions. Also, in order to consider the reversion behaviour of NR in modelling some studies were done by Ding and Leonov <sup>[53, 54]</sup> and Fan et al. <sup>[55]</sup>.

In the literature, phenomenological models for characterization of thermoset curing are used by many researchers. Kamal and Sourour <sup>[56]</sup> used DSC to characterize curing of general purpose polyester and proposed a model for the kinetics of curing. The model gave results which were seen to be in good agreement with the experimental data. Further study <sup>[57]</sup> on this model showed that the kinetic model describes the cure kinetics of both epoxy and unsaturated polyester systems adequately. This model, also known as Kamal-Sourour model (Eqn. 2.4.1) is now widely used to study the kinetics of thermosets and is seen as one of the first models to accurately define autocatalytic cross linking reactions. In Eqn. 2.4.1,  $dc/dt$  is the reaction rate,  $c$  is degree of cure,  $m$  and  $n$  are order of reactions,  $k_1$  and  $k_2$  are rate constants,  $E_1$  and  $E_2$  are activation energies,  $a_1$  and  $a_2$  are frequency factors,  $R$  is the universal gas constant and  $T$  is the processing temperature.

$$\frac{dc}{dt} = (k_1 + k_2 c^m)(1 - c)^n \quad (2.4.1)$$

$$\text{where } k_1 = a_1 \exp\left(-\frac{E_1}{RT}\right) \text{ and } k_2 = a_2 \exp\left(-\frac{E_2}{RT}\right)$$

Patridge and Karkanis <sup>[58]</sup>, developed a procedure to model the kinetics of curing for epoxy resin. DSC was used to obtain data in both isothermal and dynamic modes. They used the Kamal-Sourour model but in order to account for the diffusion effects for the post vitrification stages, the model was modified by

using two different reaction orders;  $n_1$  and  $n_2$  (Eqn. 2.4.2). Activation energy was calculated using Arrhenius equation. The model provided an accurate fit for all the cure temperatures used.

$$\frac{dc}{dt} = k_1(1-c)^{n_1} + k_2c^m(1-c)^{n_2} \quad (2.4.2)$$

Cough and Chang <sup>[59]</sup> studied the kinetics of sulfur vulcanization for different rubbers using rheometer and DSC. They used first-order kinetics together with the Arrhenius equation to model the reaction (Eqn. 2.4.3). They also investigated the relationship of the structure of a rubber and the vulcanization reactivity and reported that vulcanization rate increases proportionally to the number of allylic hydrogen in the repeat units.

$$\ln\left(\beta \frac{dc}{dt}\right) = \ln k_0 - \frac{E}{RT} + \ln(1-c); \quad \text{where } \beta = \frac{dT}{dt} \quad (2.4.3)$$

Isayev and Deng <sup>[60]</sup> proposed a non-isothermal vulcanization kinetic model. They used it particularly for cure process during rubber injection molding and reported that it can be used for any non-isothermal processing operations. DSC was used to study cure kinetics in both isothermal and non-isothermal modes. The proposed model considers vulcanization as a two-step process involving an induction period and a main reaction period. An  $n^{\text{th}}$  order kinetic equation, along with Kamal-Sourour's equation was used to develop an empirical model to describe cure kinetics as a function of cure time. Equations (2.4.4) and (2.4.5) describe the induction and vulcanization periods. Eqn. 2.4.5 was derived from Eqn. 2.4.6. The predicted data were compared with the experimental data for induction time and rate of vulcanization from non-isothermal DSC and a good agreement was observed.

$$\bar{t} = \int_0^t dt/t_i(T) \quad (2.4.4)$$

$$\frac{d\alpha}{dt} = \frac{n}{k} t^{-1-n} \alpha^2 \quad (2.4.5)$$

$$\alpha = \frac{kt^n}{1 + kt^n} \quad \text{where } k(T) = k_0 \exp\left(-\frac{E}{RT}\right) \quad (2.4.6)$$

Where  $\bar{t}$  is dimensionless time,  $t_i(T)$  is the dependence of induction time on temperature,  $\alpha$  is the degree of cure,  $n$  is the order of reaction,  $k$  is rate constant,  $E$  is activation energy,  $R$  is the universal gas constant,  $T$  is temperature.

Arrillaga et al. <sup>[51]</sup> used three different characterization techniques, DSC, MDR and ODR and employed the Isayev (Eqn.2.4.6) and Kamal (Eqn. 2.4.1) models for describing the cure kinetics of acrylonitrile butadiene rubber (NBR) and EPDM. They also used the Claxton-Liska model (Eqn. 2.4.7) to characterize the induction period. After characterization by the above mentioned techniques, a software package (Grace software) was used to determine the constants for the two models. Kaleidagraph and Sigma plot softwares were used to later crosscheck the estimated parameters predicted by the Grace software. Finally, the predicted data were compared with experimental data and it was reported that the “m” and “n” values are simply the averages of all “m” and “n” values that were determined at each temperature. So both models fit the experimental data only at certain temperatures at which the “m” and “n” values are similar to their mean values. A similar approach was taken by Khang et al. <sup>[61]</sup>. They also used Claxton-Liska (2.4.7) and Ding-Isayev (2.4.6) models along with curve fitting software to define the kinetic parameters.

$$t_s = t_0 \exp\left(\frac{T_0}{T}\right) \quad (2.4.7)$$

where,  $t_s$  is scorch time,  $t_0$  and  $T_0$  are material constants and  $T$  is absolute temperature .

Mansilla and Marzocca <sup>[62]</sup> also studied the cure kinetics of NR/SBR blends with the means of rheometer tests (MDR) and the Kamal-Sourour model was used for describing the cure kinetics. They used sulfur and TBBS (accelerator) cure system for the blends which were prepared by two different methods, mechanical mixing and solution blending. They reported that the rheometer curves were successfully described by the Kamal-Sourour model and that the cure rate depends on the blend composition and can be fitted by a mixture law. Lee and Hong <sup>[63]</sup> studied the cure kinetics of silicone rubber using DSC. They used the Kissinger, Ozawa, Flynn-Wall-Ozawa and the Friedman methods to calculate the kinetic

parameters of reaction. The Chang method was used to determine the order of reaction and also to improve the accuracy of the estimation. The modified-Chang method along with autocatalytic Kamal-Sourour models was used to describe the cure kinetics. The heat data from the kinetic parameters estimated was then compared with experimental data and it was seen that they fitted well the experimental data.

Hernandez-Ortiz and Osswald <sup>[64]</sup> developed a technique to use Kamal-Sourour model to fit dynamic DSC data. The estimated parameters do not necessarily have a physical meaning. They are mathematical expressions that fit the experimental data. Later, in order to have a better insight into the vulcanization reaction of silicone rubber, Osswald et al. <sup>[65]</sup> used the Kissinger and Arrhenius model to determine the activation energy, so that physically meaningful activation energy can be found. The rest of the parameters for the Kamal-Sourour model was then determined mathematically using the same method proposed by Hernandez-Ortiz and Osswald <sup>[64]</sup>. The total heat of reaction and peak temperature for vulcanization reaction of each sample was measured using dynamic DSC scans from 20 to 150 °C, also multiple scan rates were used to be able to determine the activation energy and have an insight into the effect of time and temperature on the vulcanization reaction. The kinetic parameters were first expanded with a quadratic dependence on temperature and later least squares estimation algorithm developed by Marquardt was used to fit the parameters in the model to the experimental DSC data and estimate the fitted constants. It was also reported that the estimated parameters were highly temperature dependent and they model the experimental data well only when the temperature conditions used for modelling are same as in the experimental data. Also, the model was very sensitive to the estimated parameter values.

Modelling of cure kinetics of DR was not been touched upon by many. Isayev et al. <sup>[60]</sup> reported that their study was the first attempt to look at the development of such a kinetic approach for DR. In their study, they devulcanized ground rubber tire using a coaxial ultrasonic devulcanization reactor at different amplitude. Advanced polymer analyzer (APA 2000) was used to cure the sample at different isothermal

conditions. Also, samples were non-isothermally cured to verify the ability of the model to predict non-isothermal curing behavior including reversion. Two different kinetic models were used in their study. Isayev-Deng's <sup>[60]</sup> kinetic model based on reduced time approach was used at first but the model was unable to predict the reversion behavior of the sample, so another model was used which was based on cure reversion at high temperature. A simple reaction mechanism was proposed to describe reversion and also an induction time function was used to predict isothermal induction times. The data from APA were converted to degree of cure as a function of time and Sigma plot was used for curve fitting using a nonlinear least-squares regression model. It was seen that the kinetic model fits the data quite accurately at intermediate temperatures as four different temperatures were used for fitting. Prediction for non-isothermal curing behavior and experimental data also showed close agreement for ultrasonically devulcanized rubber. Later, cross-linking density and gel fraction of the samples were analyzed and correlation between crosslink density and degree of cure of DR during revulcanization was analyzed and found to be independent of the time-temperature history.

## **2.5 Summary**

- Recycling of scrap rubber is an important step as it not only reduces environmental problems but also helps in recovering a usable resource.
- Once the material is devulcanized, it can be reprocessed and revulcanized to get a usable product. But the vulcanization process of DR differs from virgin rubber so modelling of this reaction can help in better understanding and also in reduction of time required to choose an appropriate cure system.
- Kinetic models are generally categorized into mechanistic and phenomenological models. In this study, the phenomenological approach was used.

- A number of characterization techniques have been described in literature like DSC, MDR, ODR, etc. From those techniques non-isothermal DSC was selected to characterize vulcanization reactions for this study.
- Also, from the different kinetic models used for describing different thermosets, the Kamal-Sourour model (Eqn. 2.4.1) along with the fitting technique developed by Hernandez-Ortiz and Osswald <sup>[64-65]</sup> was used for modelling the vulcanization reaction of DR. DR used in this study was the DR obtained from the devulcanization method developed by Tzoganakis <sup>[42]</sup>.

## Chapter 3

### EXPERIMENTAL

#### 3.1 Materials

- All the materials that were used in the experiments are tabulated in Table 3.1 with their suppliers.

**Table 3.1: List of materials used.**

Materials	Supplier	Comments
Natural Rubber (NR)	AirBoss of America	Rubber
Devulcanized Rubber (DR)	Tyromer Inc.	Rubber
Master batch (Truck Tire Tread)	AirBoss of America	Rubber
Sulphur (S)	Cooper Standard	Cross linking Agent (Used for curing)
N-tert-butyl-2-benzothiazyl sulfenamide (TBBS)	Sunboss chemicals	Accelerator (Used for curing)
Zinc oxide (ZnO)	Sigma Aldrich	Activator (Used for curing)
Stearic acid (St. A)	Fisher Scientific	Activator (Used for curing)

- The list of equipment used along with their suppliers can be found in Table 3.2.

**Table 3.2: List of equipment used.**

Equipment	Supplier
Batch Mixer	Rheomix 3000 attached to Rheocord 90 (Haake)
DSC Q2000	TA Instruments

### 3.2 Design of Experiments

To study the effect of dosages of sulfur and accelerator on total heat of reaction and peak temperature, a two-level factorial design was used with three centre point replicates (C1/C2/C3). The variables studied were sulphur and TBBS concentrations. The two levels, i.e. the minimum and maximum dosage (0.5 and 2.5phr), for the design were chosen based on some previous work done on DR by our research group. Thus, based on this design seven samples (i.e.  $2^2 + 3$  centre point replicates =7 samples) were mixed according to the formulations shown in Tables 3.3 and 3.4.

**Table 3.3: Formulation for NR samples**

Ingredients	Dosages (phr/gm)									
	Sample A		Sample B		Sample C1/C2/C3		Sample D		Sample E	
	phr	gm	phr	gm	phr	gm	phr	gm	phr	gm
<b>Natural Rubber (NR)</b>	100	200	100	200	100	200	100	200	100	200
<b>Sulphur</b>	0.5	1	2.5	5	1.5	3	0.5	1	2.5	5
<b>TBBS</b>	0.5	1	0.5	1	1.5	3	2.5	5	2.5	5
<b>Zinc Oxide</b>	3	6	3	6	3	6	3	6	3	6
<b>Stearic Acid</b>	1	2	1	2	1	2	1	2	1	2

**Table 3.4: Formulation for DR samples**

Ingredients	Dosages (phr/gm)									
	Sample A		Sample B		Sample C1/C2/C3		Sample D		Sample E	
	phr	gm	phr	gm	phr	gm	phr	gm	phr	gm
Devulcanized Rubber (DR)	100	200	100	200	100	200	100	200	100	200
Sulphur	0.5	1	2.5	5	1.5	3	0.5	1	2.5	5
TBBS	0.5	1	0.5	1	1.5	3	2.5	5	2.5	5
Zinc Oxide	3	6	3	6	3	6	3	6	3	6
Stearic Acid	1	2	1	2	1	2	1	2	1	2

### 3.3 Methods

#### 3.3.1 Mixing: Batch Mixer

Mixing was carried out for different samples using the batch mixer (Figure 3.1) at room temperature with rotor speed set to 60 rpm.

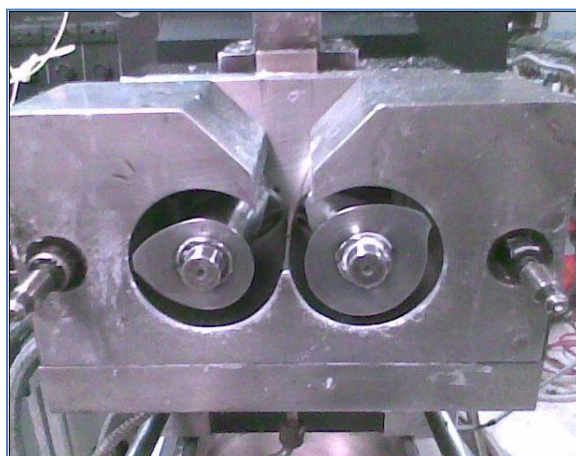


**Figure 3.1: Batch mixer used for mixing.**

First, the rubber was added into the batch mixer and after the torque became stable the rest of the ingredients were added. Mixing was carried out until a stable torque was achieved. In this study, different rubbers were used. First, NR samples (Table 3.3) were mixed and characterized, followed by DR samples (Table 3.4). Additionally, blends of DR and a master batch compound (Table 3.5) were mixed and characterized (formulation decided based on the composition of the pre-mixed master batch).

**Table 3.5: Formulations for blends of master batch compound (Truck Tire Tread compound) and DR.**

Ingredients	Dosages (gm)					
	10%		20%		30%	
	phr	gm	phr	gm	phr	gm
Master batch compound	148.86	180	132.32	160	115.78	140
Devulcanized Rubber	16.54	20	33.08	40	49.62	60
Sulphur	0.14	0.17	0.28	0.34	0.42	0.51
TBBS	0.1	0.12	0.2	0.24	0.3	0.36
Zinc Oxide	0.5	0.60	1	1.21	1.5	1.81
Stearic Acid	0.1	0.12	0.2	0.24	0.3	0.36

### 3.3.2 Characterization via DSC

After the samples were mixed with curatives, their vulcanization behavior was studied using DSC. The heat released during the vulcanization reaction (as it is exothermic in nature) was captured using DSC.

A heat flux DSC was used for the experiments. The sample and reference pans were first prepared. A sealed aluminum pan (an empty pan with lid) was used as a reference. Samples were weighed (around 7-9mg) and sealed in an aluminum pan with lid. Once the sample and reference pans were ready, they were placed in the sample and reference trays respectively, and individual samples were then scanned at

different scanning rates from room temperature to 250 °C under nitrogen atmosphere. Different scan rates were used to get a better understanding of the effect of time and temperature on vulcanization reaction. Some scan rates were also used to validate the model. The different scan rates used were 5, 10, 15, 18, 20, 22.5, 25, 30, 35 and 40 °C/min.

During the scanning of each sample, the computer attached to the DSC recorded the temperature, time and heat flow for the sample. Representative sample heat flow data are shown in the thermogram in Figure 3.2. The data were later used to fit the kinetic model and also analyzed to see the effect of curatives on the vulcanization reaction.

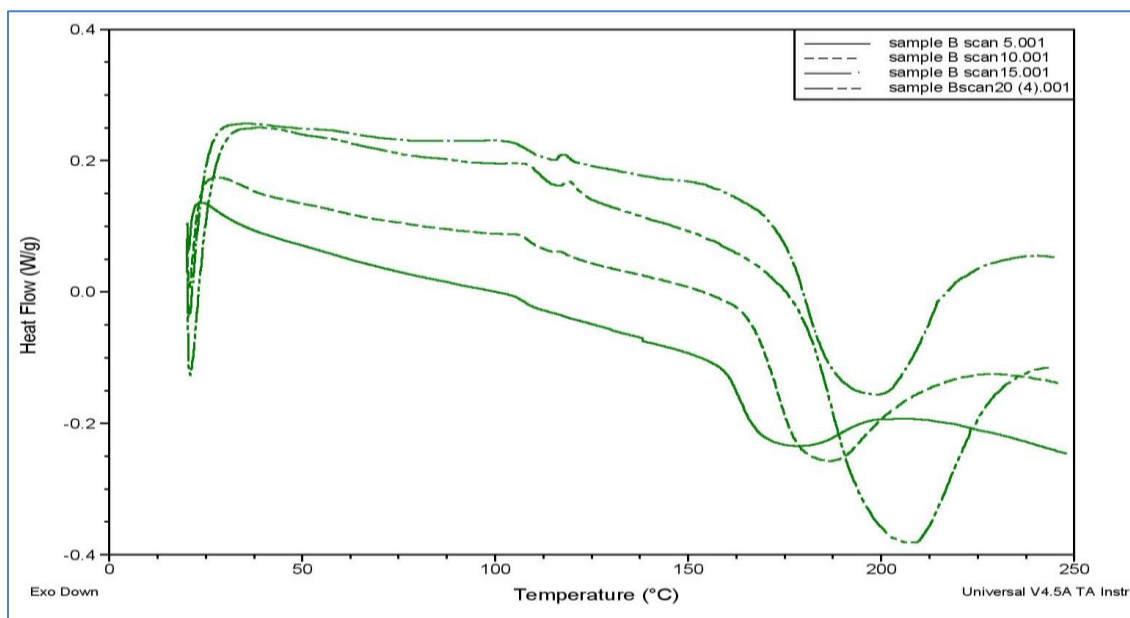


**Figure 3.2: DSC thermogram for NR sample B at different scan rates.**

## Chapter 4

### Kinetic Models

Vulcanization is a chemical reaction and its characterization involves kinetic parameters. As mentioned in the literature review due to the complex reactions involved in vulcanization, phenomenological models are used in this study. These models are simple to compute and are based on the rate of reaction <sup>[65]</sup>.

$$\frac{dc}{dt} = k(T)f(c) \quad (4.1)$$

where  $c$  is the degree or extent of vulcanization,  $k$  is the rate constant as a function of temperature and  $f(c)$  is a function of the degree of vulcanization. The degree of vulcanization can be measured by tracking the concentration of reactants and products but that process is difficult to monitor and also involves costly spectroscopic analysis. However, as the vulcanization reaction is exothermic in nature, it can be assumed that the heat released during the reaction is proportional to the degree of vulcanization. This heat released can be related to the degree of vulcanization (as shown in Eqns. 4.2-4.5). DSC is a method of thermal analysis and it can record the heat released during the reaction. In this method, it is assumed that each bond releases the same amount of energy and the heat released is only due to formation of cross links (not side reactions). The heat flow data obtained from DSC can be related to the degree of vulcanization by the following equations. The heat released during vulcanization can be calculated by <sup>[64, 65]</sup>,

$$Q = \int_0^\tau \dot{Q} dt \quad (4.2)$$

where  $Q$  is the heat released up to time  $\tau$  and  $\dot{Q}$  is the instantaneous rate of heat released by the sample.

The total heat of reaction  $Q_T$ , equals to,

$$Q_T = \int_0^{\tau_{final}} \dot{Q} dt \quad (4.3)$$

where  $\tau_{final}$  is the time at which the reaction is complete. The rate of reaction,  $dc/dt$  is then given as,

$$\frac{dc}{dt} = \dot{Q}/Q_T \quad (4.4)$$

and finally the degree of vulcanization ( $c$ ) is obtained as below.

$$c = \frac{Q}{Q_T} \quad (4.5)$$

Kinetic models relate the reaction rate to temperature and degree of reaction. The main challenge in modelling the reaction is to take DSC data and fit models that will describe the vulcanization reaction of the rubber used <sup>[65]</sup>. To model the vulcanization reaction of devulcanized rubber, the Kissinger <sup>[66, 67]</sup> model along with the Arrhenius <sup>[68]</sup> equation and Kamal-Sourour model <sup>[56, 57]</sup> were used. The technique developed by Hernandez-Ortiz and Osswald <sup>[64, 65]</sup> for using the Kamal-Sourour model to fit to the dynamic DSC data was used in this study. First, the Kissinger equation along with the Arrhenius equation were used to estimate the activation energy, which was later used to determine the rest of the five parameters for the Kamal-Sourour model by least squares estimation.

## 4.1 Calculation of Activation Energy

### 4.1.1 Arrhenius Model

This equation was proposed by Svante Arrhenius in 1889 and it describes the temperature dependence of chemical reaction rates <sup>[68]</sup>. According to this model a reaction rate constant is the product of a pre-exponential factor (frequency) 'a' and an exponential term. It considers that an energy barrier hinders the progress of a reaction and a minimum energy is required to overcome this barrier which is known as activation energy, E. The rate constant ( $k$ ) can be defined as follows by the Arrhenius model,

$$k(T) = a e^{-\left(\frac{E}{RT}\right)} \quad (4.6)$$

where a is the frequency factor, E is the activation energy, T is the absolute processing temperature and R is the universal gas constant.

#### 4.1.2 Kissinger Model <sup>[66, 67]</sup>

This n<sup>th</sup> order model can be defined as follows,

$$\frac{dc}{dt} = k(1 - c)^n \quad (4.7)$$

where k is the rate constant defined by Arrhenius equation, dc/dt is the reaction rate, c is the degree of vulcanization and n is the order of reaction.

#### Activation Energy Calculation <sup>[65]</sup>

In the case of heat activated reactions, if the heating rate ( $\dot{T}$ ) is varied, the position of the peak observed in the DSC thermogram also varies. The rate of reaction (dc/dt) increases with temperature and reaches a maximum value and comes back to zero as the reactants are consumed. The temperature, at which the reaction rate reaches a maximum value, is termed as peak temperature ( $T_{peak}$ ). Dynamic DSC measurements at different heating rates are used to determine the activation energy of the material by using equation 4.8. This equation was derived for activation energy by combining both equations 4.6 and 4.7.

$$-\frac{E}{R} = \frac{d\left(\ln \frac{\dot{T}}{T_{peak}^2}\right)}{d\left(\frac{1}{T}\right)} \quad (4.8)$$

A graph (Figure 4.1) was generated using Eqn. 4.8 with different heating rates ( $\dot{T}$ ) and  $T_{\text{peak}}$ . The slope of the line corresponds to the negative ratio of activation energy and universal gas constant ( $-E/R$ ). As the value of  $R$  is known, the activation energy can be thus calculated from the slope of the line.

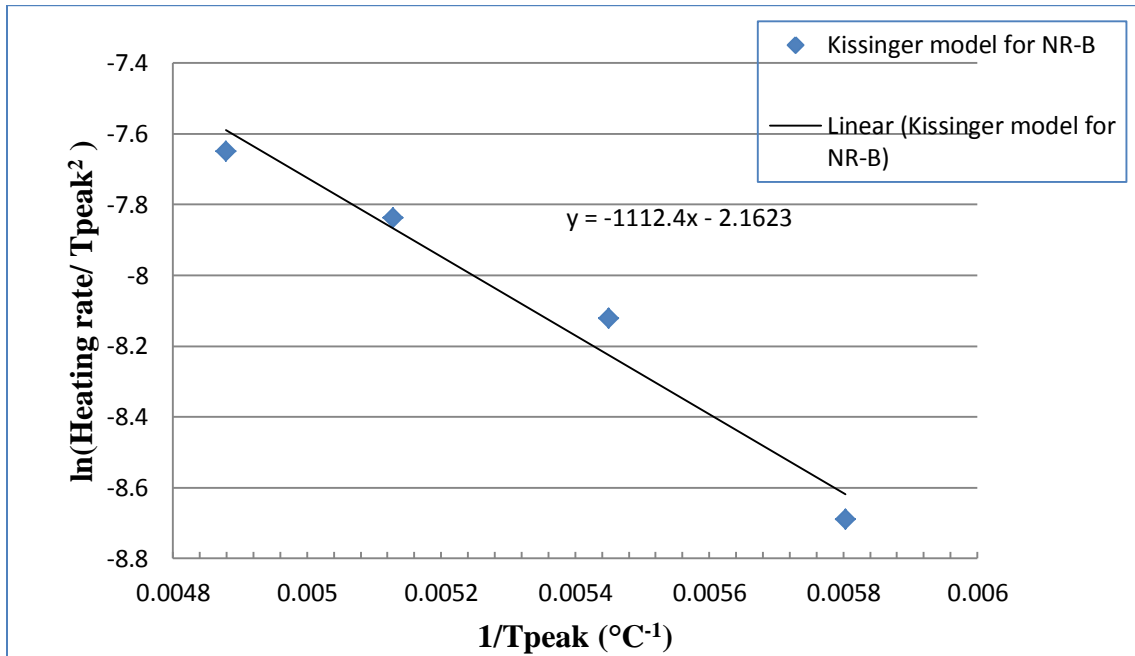


**Figure 4.1: Kissinger Model for NR sample B for activation energy calculation**

## 4.2 Kamal-Sourour Model <sup>[56, 57]</sup>

The Kamal-Sourour model is considered as one of the first models to accurately define autocatalytic cross linking reactions <sup>[65]</sup>. The model can be defined as follows:

$$\frac{dc}{dt} = (k_1 + k_2 c^m)(1 - c)^n \quad (4.9)$$

$$\text{where } k_1 = a_1 \exp\left(-\frac{E_1}{RT}\right) \text{ and } k_2 = a_2 \exp\left(-\frac{E_2}{RT}\right)$$

where  $k_1$  and  $k_2$  are the rate constants and  $m$  and  $n$  are reaction orders. The rate constants can be described by Arrhenius models as shown above. The model has six parameters ( $a_1$ ,  $a_2$ ,  $E_1$ ,  $E_2$ ,  $m$  and  $n$ ) that need to be estimated. The kinetic parameters were determined in this study using the same method developed by Hernandez-Ortiz and Osswald <sup>[65]</sup>. The activation energy ( $E_1$ ) was calculated using the Kissinger and Arrhenius models and the activation energy,  $E_2$ , was estimated as a constant. The remaining parameters were expressed as polynomial functions of temperature (Eqn. 4.10 and 4.11),

$$x_i = a_{i1} + a_{i2}T + a_{i3}T^2 \quad (4.10)$$

where  $i=1, \dots, 4$  and  $a_{ij}$  are the 13 new parameters to be estimated.

$$\left. \begin{aligned} m &= a_{11} + a_{12}T + a_{13}T^2 \\ n &= a_{21} + a_{22}T + a_{23}T^2 \\ a_1 &= a_{31} + a_{32}T + a_{33}T^2 \\ a_2 &= a_{41} + a_{42}T + a_{43}T^2 \\ E_2 &= E_2 + 0 + 0 \end{aligned} \right\} (4.11)$$

According to Eqn. 4.10, the higher order terms can be neglected if the coefficient accompanying the second order term after the fitting is small or else the higher order terms must be included.

From DSC experiments, temperature, time, heat flow and sample weight data were obtained and used for the calculation of  $dc/dt$  and  $c$  for each scan rate. The model parameters were estimated by using the dependent variable vectors, temperature ( $T$ ), degree of cure ( $c$ ) and reaction rate ( $dc/dt$ ) and an initial guess matrix for the 13 constants as input to the program. FORTRAN (Formula Translating System) programming language was used in which least square estimation algorithm (modification of Lavenberg-Marquardt algorithm) was used to estimate the parameters. This algorithm tries to minimize a function that represents the difference between the experimental and estimated values of  $dc/dt$  according to the Kamal-Sourour model. The steps followed for fitting the model to the data are shown below in the form of a flow chart in Figure 4.2.

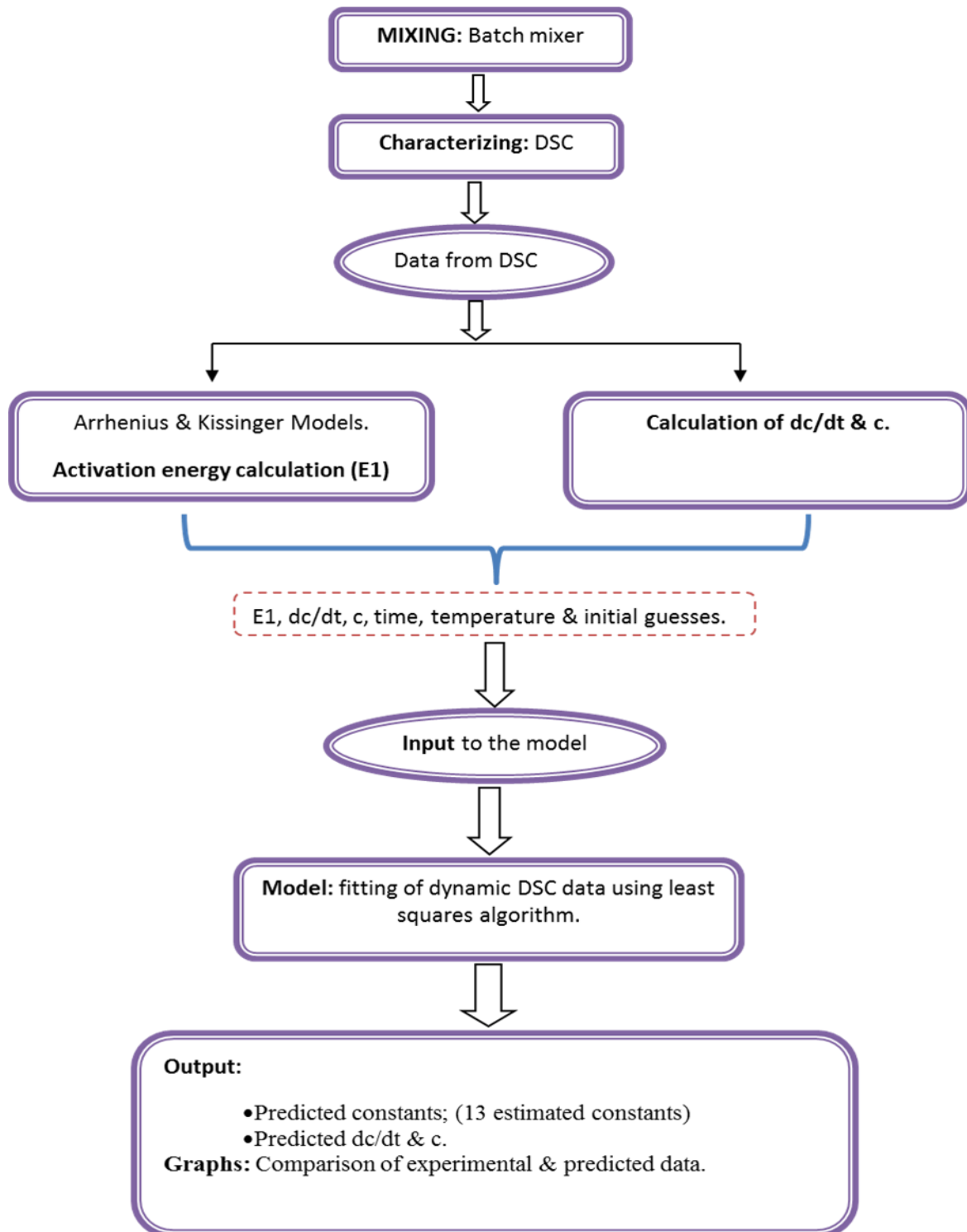


Figure 4.2: Schematic of steps followed for model fitting.

## Chapter 5

### Results and Discussion

#### 5.1 Natural Rubber and Devulcanized Rubber Samples

##### 5.1.1 DSC

Samples were scanned using DSC at different scan rates. Those scans were analyzed and peak temperature ( $T_{\text{peak}}$ ) and total heat of the reaction data for different scan rates were recorded. Results from one scan rate are shown in the tables below for all samples (Table 5.1 and 5.2) and the rest are given in Appendix A.

The objectives for performing these scans were:

- To examine the effect of cure system and scanning rates on both types of rubber samples.
- To compare the curing behavior of DR with a virgin NR rubber.
- To use the reaction heat data for estimating kinetic parameters in the Kamal-Sourour model.

#### Results for NR and DR samples:

**Table 5.1: Scans at Heating Rate of 20 °C/min for NR samples.**

Sample	Sample mass (mg)	$T_{\text{peak}}$ (°C)	Total heat of reaction (J/g)
A	7.15	202.9	12.1
B	7.16	205.0	31.9
C1	7.21	198.5	19.3
C2	7.13	198.8	19.5
C3	7.1	198.2	20.8
D	7.18	205.3	14.6
E	7.15	195.8	27.1

**Table 5.2: Scans at Heating Rate of 20 °C/min for DR samples.**

<b>Sample</b>	<b>Sample mass (mg)</b>	<b>T<sub>peak</sub> (°C)</b>	<b>Total heat of reaction (J/g)</b>
<b>A</b>	<b>7.10</b>	195.9	15.7
<b>B</b>	<b>7.15</b>	192.8	30.7
<b>C1</b>	<b>7.22</b>	190.8	27.5
<b>C2</b>	<b>7.18</b>	189.8	24.6
<b>C3</b>	<b>7.12</b>	190.2	23.9
<b>D</b>	<b>7.27</b>	188.1	21.4
<b>E</b>	<b>7.14</b>	187.5	25.7

a. **Effect of different scan rates on the curing of rubber samples:**

All the samples were scanned at different scan rates i.e. 5, 10, 15, 20 and 25°C/min. It can be seen (Figure 5.1 and 5.2) that the total heat of reaction is relatively unaffected by scan rate for all samples.

Also, with the increase in scan rate, the T<sub>peak</sub> for each sample increases (Figure 5.3 - 5.6).

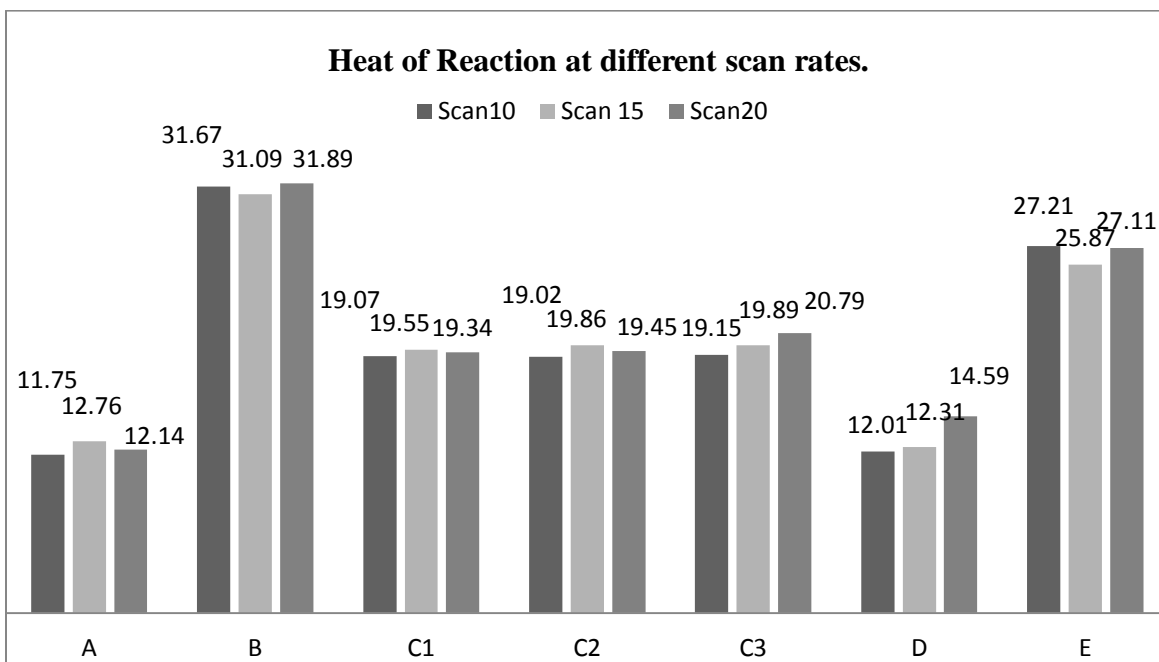


**Figure 5.1:** Graphical representation of the heat of reaction data for NR samples.

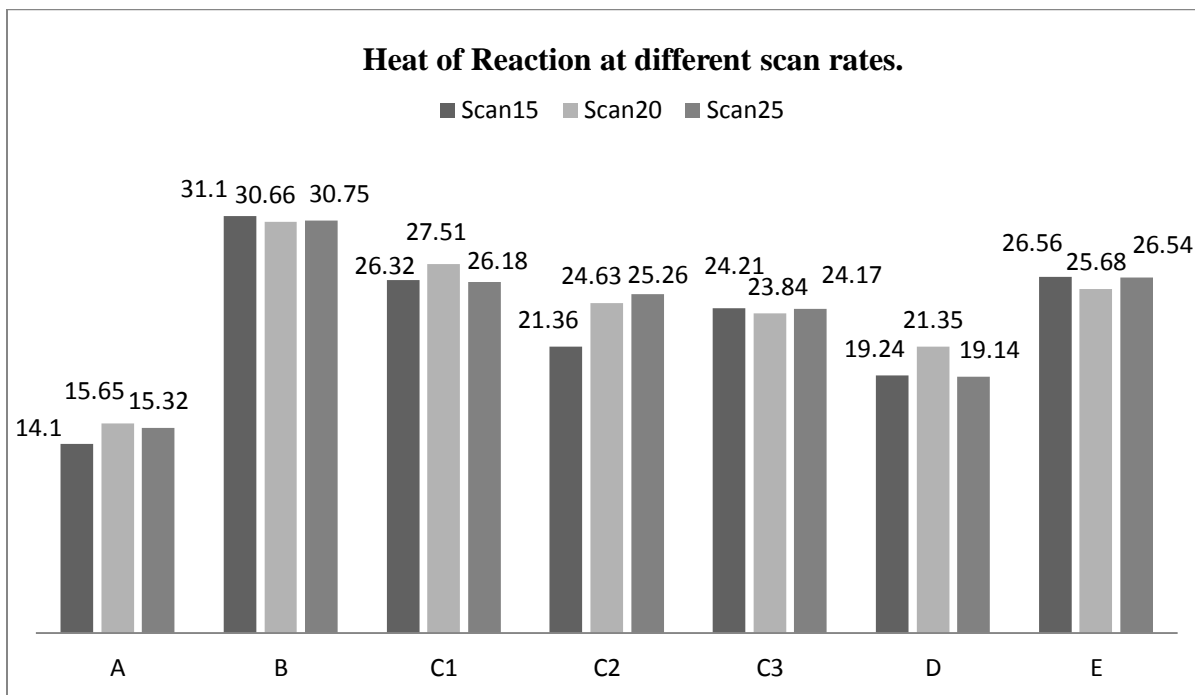


**Figure 5.2:** Graphical representation of the heat of reaction data for DR samples.

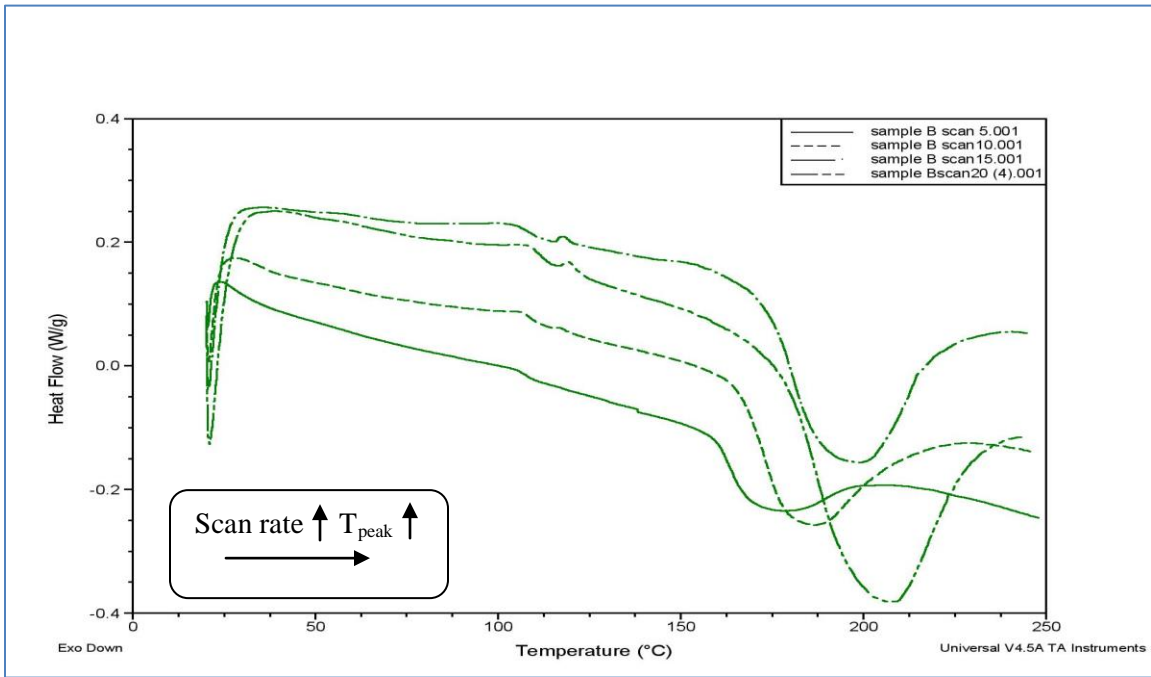


**Figure 5.3: DSC curve for NR Sample B at different scan rates.**

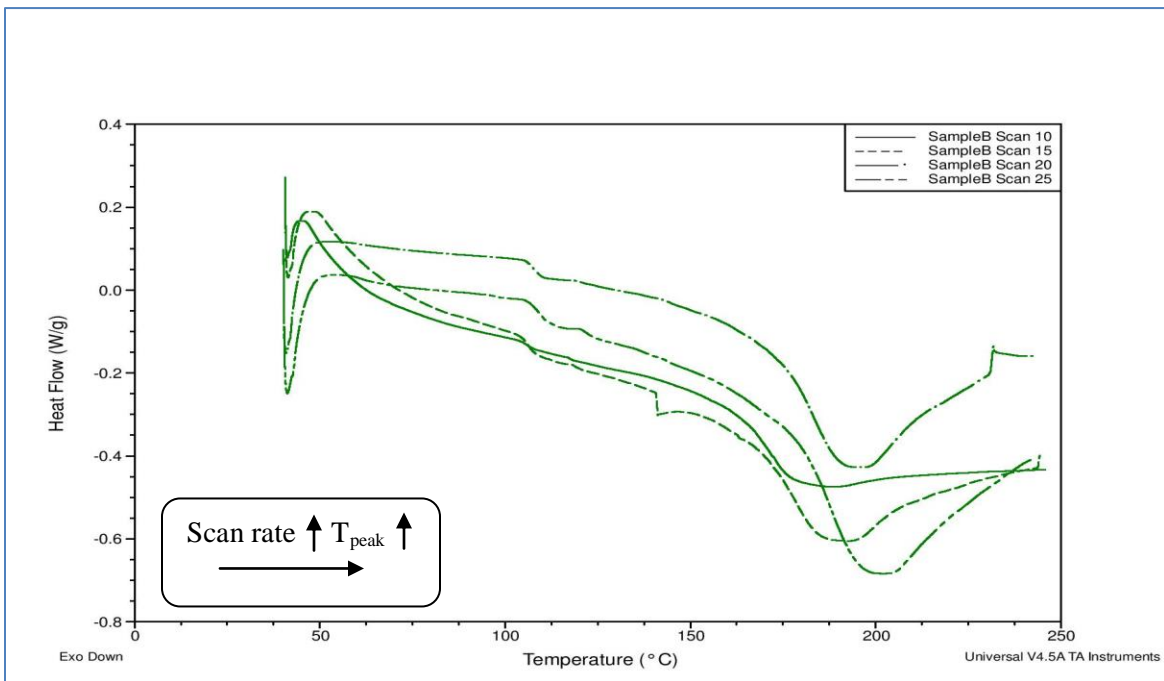


**Figure 5.4: DSC curve for DR Sample B at different scan rates.**

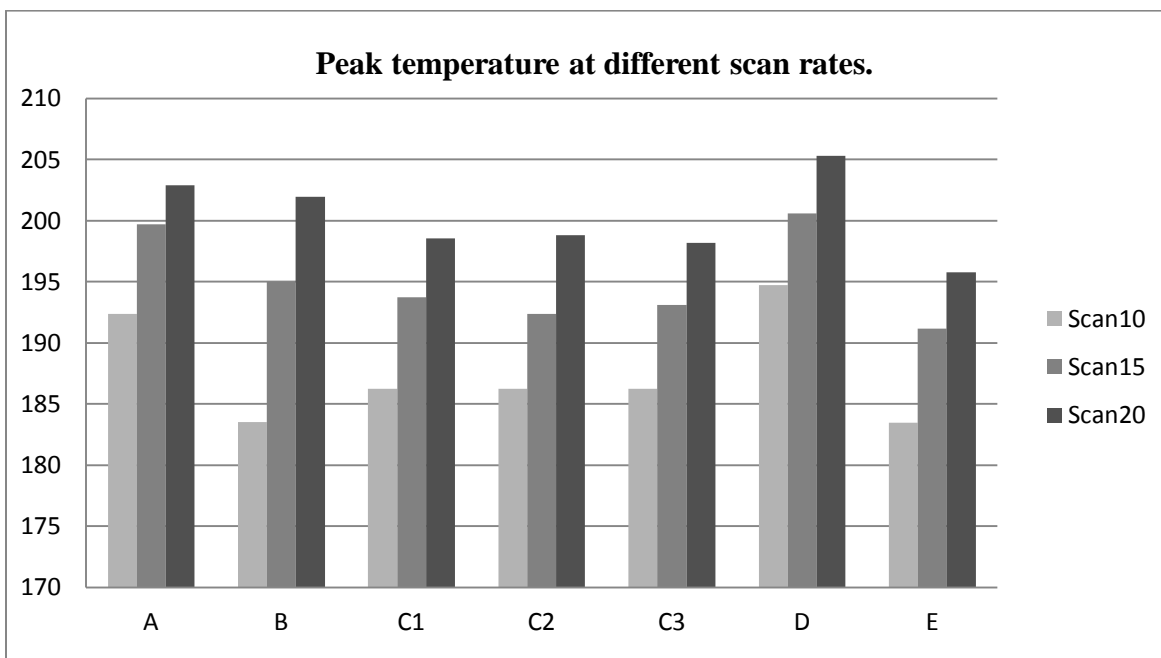


**Figure 5.5: Peak temperature of different NR samples at different scan rates.**

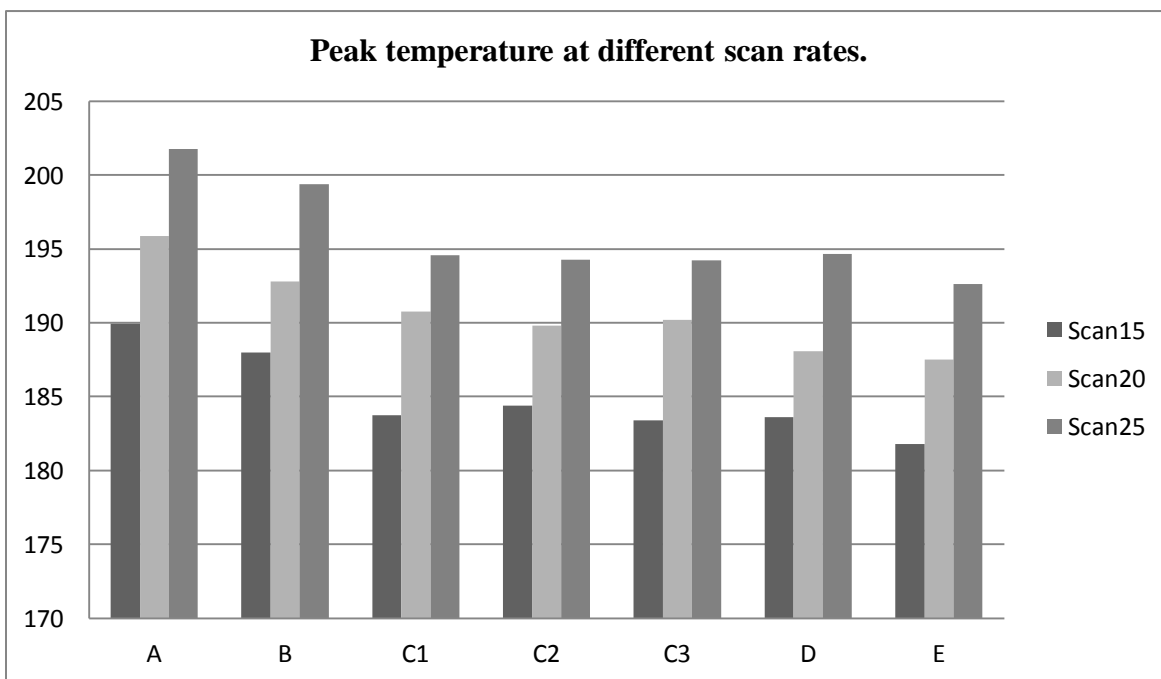


**Figure 5.6: Peak temperature of different DR samples at different scan rates.**

**b. Effect of curative composition:**

The effect of different dosages of curatives was visible in the total heat of reaction and somewhat in the peak temperature (Figure 5.1- 5.2 and 5.5-5.6). These are explained as follows:

**Total heat of reaction:**

The following trend was observed in the total heat of reaction regardless of the scan rate used for both the rubber compounds:

**Sample B > Sample E > Sample C1~C2 ~C3 > Sample D~ Sample A**

Sample B with 2.5 phr sulfur and 0.5 phr accelerator shows the highest heat of reaction in all the different scan rates, followed by sample E which contains same amount of sulfur and 2.5phr accelerator. The sulfur to accelerator ratio is higher in sample B compared to sample E. Higher heat of reaction in sample B can be due to some slow reactions that can occur over long period of vulcanization<sup>[9]</sup>. Accelerators are thought to promote mono- and di- sulfide bond<sup>[8, 59]</sup> so more number of polysulfidic bonds compared to mono- and di- sulfidic bonds in sample E can be formed compared to sample B.

Sample C (C1, C2 and C3) with equal dosages of both sulfur and accelerator shows moderate heat of reaction.

Sample A and D show almost equal amount of heat of reaction regardless of the higher dosage of accelerator in sample D comparatively.

Both natural rubber and devulcanized rubber samples show the same trend in heat of reaction. However, the magnitude of the total heat of reaction for devulcanized rubber samples was lower compared to natural rubber samples, which is likely due to the presence of a lesser amount of unsaturation available for cross linking.

### **Peak temperature:**

The peak temperature ( $T_{\text{peak}}$ ) for NR samples (Figure 5.5) was highest in the case of sample D which has highest accelerator to sulfur ratio (2.5 phr/ 0.5phr) followed by samples A, B, C, and E, respectively. This may be due to the fact that increasing the accelerator dosages speeds up the reaction, leading to a narrower peak with high  $T_{\text{peak}}$ . But the trend of  $T_{\text{peak}}$  in the case of DR (Figure 5.6) is different; the highest  $T_{\text{peak}}$  was observed in Sample A (0.5 phr), followed by samples B, C, D and E, respectively. The modified chemical structure of DR and presence (if) of any other ingredients from before could be the reason behind this difference.

### **5.1.2 Statistical Analysis**

Statistical analysis was performed to determine the influence of sulphur and TBBS on total heat of reaction. Analysis of variance was done using Statistica software. The independent variables which have significant effects on the dependent variable were identified and reported for both rubber types. ANOVA tables (Table 5.3-5.6) and Pareto charts (Figure 5.7-5.10) for some of the samples at different scan rates are reported here.

#### **➤ Results for NR samples:**

**Table 5.3: ANOVA at a Scan rate 15°C/min for Natural Rubber Samples;**

**$R^2=0.99624$ ; 2\*\*(2-0) design**

<b>Factor</b>	<b>SS</b>	<b>df</b>	<b>MS</b>	<b>F</b>	<b>p</b>
<b>(1)Sulfur</b>	<b>254.2430</b>	<b>1</b>	<b>254.2430</b>	<b>753.8897</b>	<b>0.000106</b>
<b>(2)TBBS</b>	<b>8.0372</b>	<b>1</b>	<b>8.0372</b>	<b>23.8322</b>	<b>0.016433</b>
<b>1 by 2</b>	<b>5.6882</b>	<b>1</b>	<b>5.6882</b>	<b>16.8669</b>	<b>0.026134</b>
<b>Error</b>	1.0117	3	0.3372		
<b>Total SS</b>	268.9802	6			

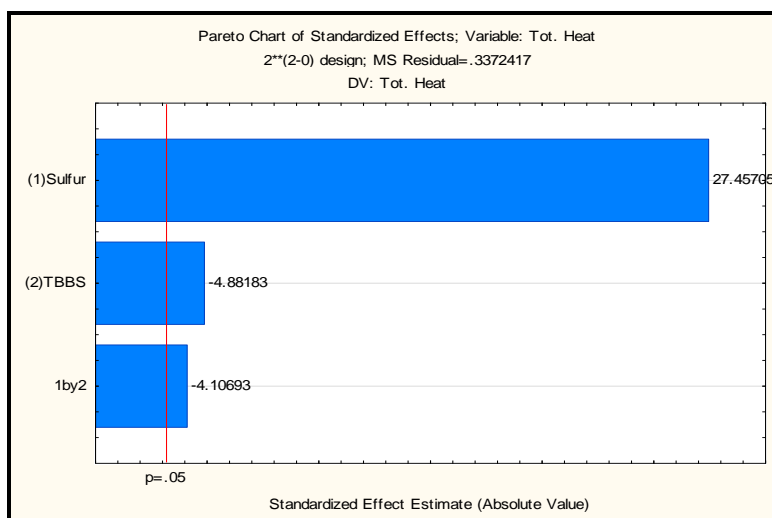


Figure 5.7: Pareto chart for Scan rate 15°C/min.

Table 5.4: ANOVA at a Scan rate 20°C/min for Natural Rubber Samples;  $R^2=0.98023$ ; 2\*\*(2-0) design.

Factor	SS	df	MS	F	p
<b>(1)Sulfur</b>	<b>260.3382</b>	<b>1</b>	<b>260.3382</b>	<b>140.9161</b>	<b>0.001285</b>
<b>(2)TBBS</b>	1.3572	1	1.3572	0.7346	0.454396
<b>1 by 2</b>	13.0682	1	13.0682	7.0736	0.076363
<b>Error</b>	5.5424	3	1.8475		
<b>Total SS</b>	280.3061	6			

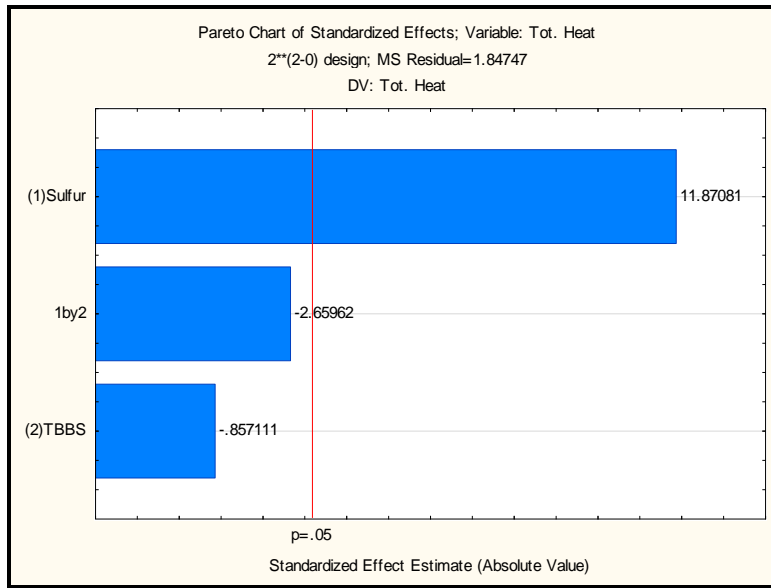


Figure 5.8: Pareto chart for Scan rate 20°C/min.

➤ Results for DR samples:

Table 5.5: ANOVA at a Scan rate 20°C/min for Devulcanized Rubber Samples;  $R^2=0.97918$ ;

2\*\*(2-0) design

Factor	SS	df	MS	F	p
(1)Sulfur	90.9162	1	90.91623	127.5678	0.001488
(2)TBBS	1.1342	1	1.13423	1.5915	0.296286
1 by 2	8.4972	1	8.49723	11.9228	0.040849
Error	2.1381	3	0.71269		
Total SS	102.6857	6			

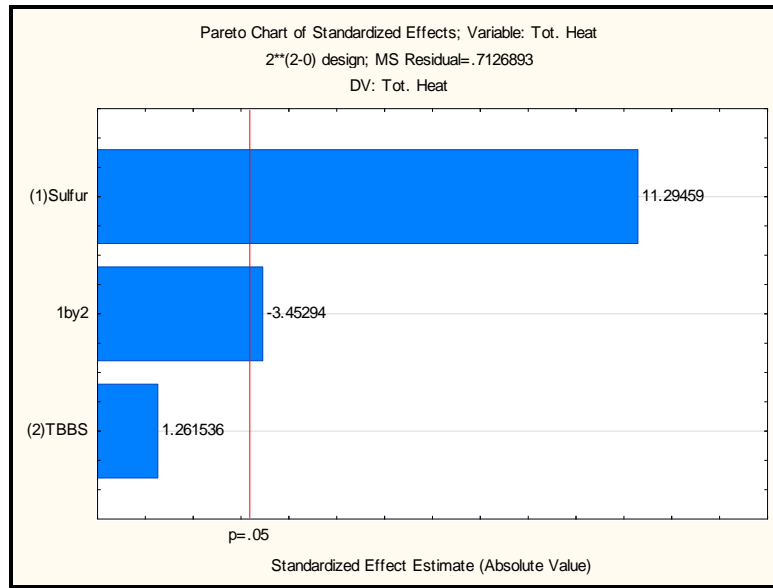


**Figure 5.9: Pareto chart for Scan rate 20°C/min.**

**Table 5.6: ANOVA at a Scan rate 25°C/min for Devulcanized Rubber Samples;  $R^2=0.96175$ ;  
 2\*\*(2-0) design**

Factor	SS	df	MS	F	p
(1)Sulfur	69.3056	1	69.30563	45.35839	0.006684
(2)TBBS	17.1810	1	17.18103	11.24445	0.043952
1 by 2	28.7832	1	28.78323	18.83773	0.022573
Error	4.5839	3	1.52796		
Total SS	119.8537	6			

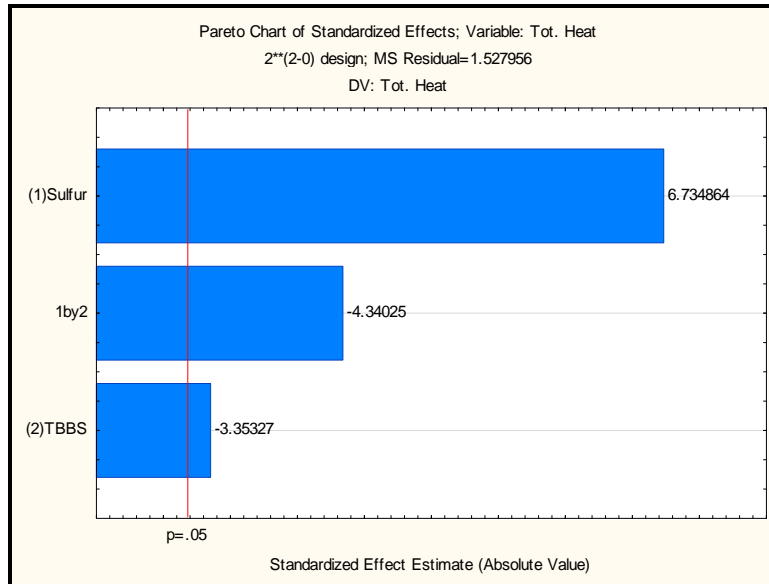


**Figure 5.10: Pareto chart for Scan rate 25°C/min.**

From the ANOVA and Pareto charts it can be seen that: (A brief summary of the results is also shown below in Table 5.7.)

- I. Sulfur has a significant effect on the dependent variable (total heat of reaction) at all the different scan rates.
- II. The independent variable TBBS and interaction between sulfur and TBBS, becomes significant only at higher scan rates, which may be due to the fast rate of vulcanization in which accelerator (TBBS) plays important role.
- III. In the case of the devulcanized rubber samples at a scan rate of 20°C/min, sulfur and interaction between sulfur and TBBS was significant. But at a higher scan rate it was observed that even TBBS becomes significant.

**Table 5.7: Significant Variables at different scan rates.**

<b>For Natural rubber samples-:</b>	
<b>Scan Rate</b>	<b>Significant Variables</b>
<b>5°C/min</b>	Sulfur
<b>10°C/min</b>	Sulfur
<b>15°C/min</b>	Sulfur, TBBS, Sulfur*TBBS
<b>20°C/min</b>	Sulfur
<b>For Devulcanized rubber samples-:</b>	
<b>20°C/min</b>	Sulfur, Sulfur*TBBS
<b>25°C/min</b>	Sulfur, TBBS, Sulfur*TBBS

Regression co-efficients for the total heat of reaction at different scan rates were calculated (Values for scan rate of 15°C/min only are shown in Table 5.8).

**Table 5.8: Regression Coefficients at 15°C/min for Natural Rubber Samples.**

<b>Factors</b>	<b>Regression Coefficients</b>
<b>Mean/Interc.</b>	7.674375
<b>(1)Sulfur</b>	4.880625
<b>(2)TBBS</b>	0.185625
<b>1 by 2</b>	-0.298125

Using these regression co-efficients, a regression model was built for the total heat of reaction (Eqn. 5.1) and the significant terms are highlighted in the Eqn. 5.1:

$$\text{Total Heat of Reaction} = 7.674375 + \mathbf{4.880625(Sulfur)} + 0.185625 (TBBS) - \mathbf{0.298125 (Sulfur * TBBS)} \quad (5.1)$$

The proposed model was evaluated using a plot of predicted versus observed values which is shown in figure 5.11.

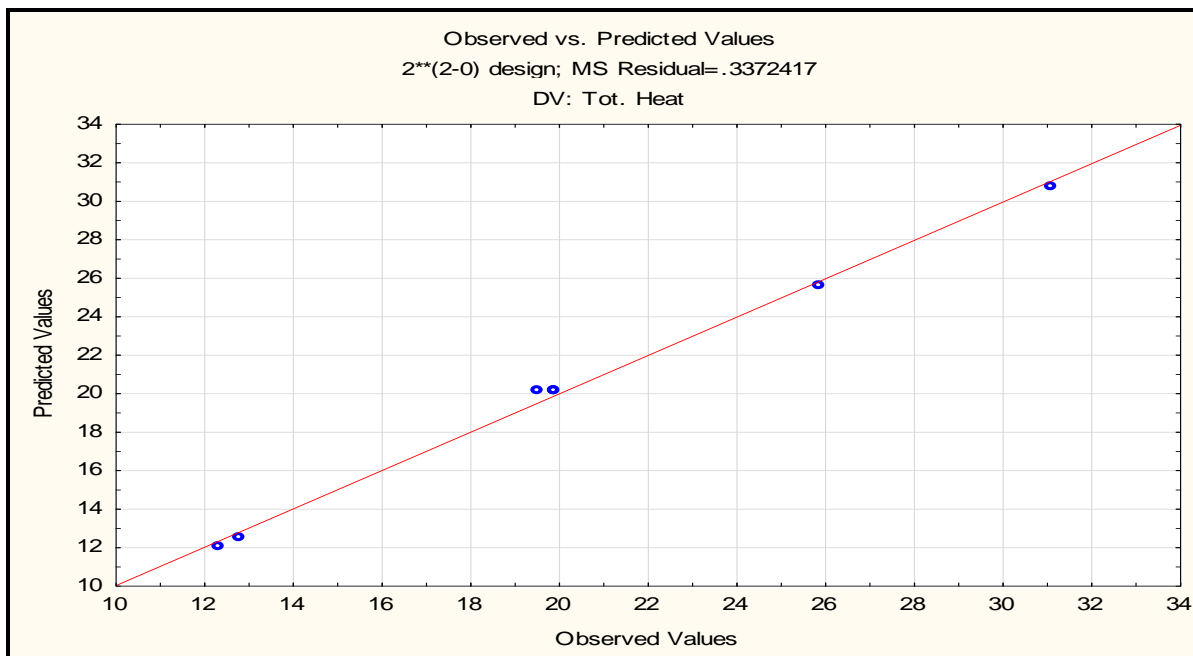
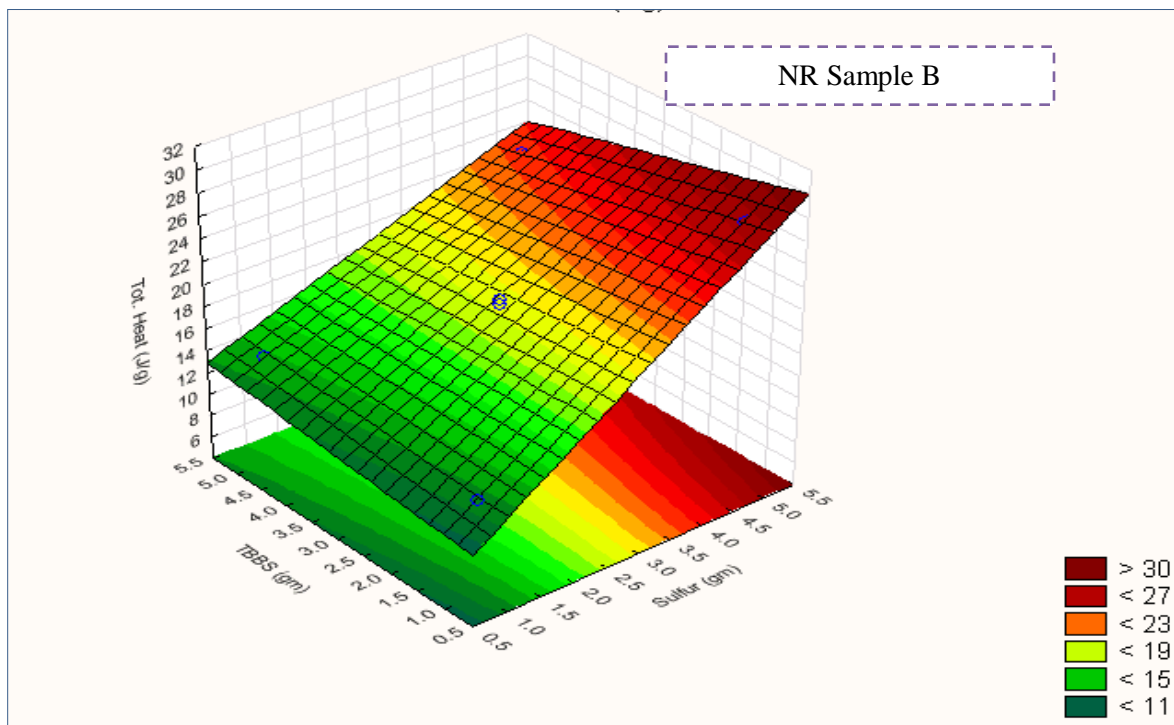
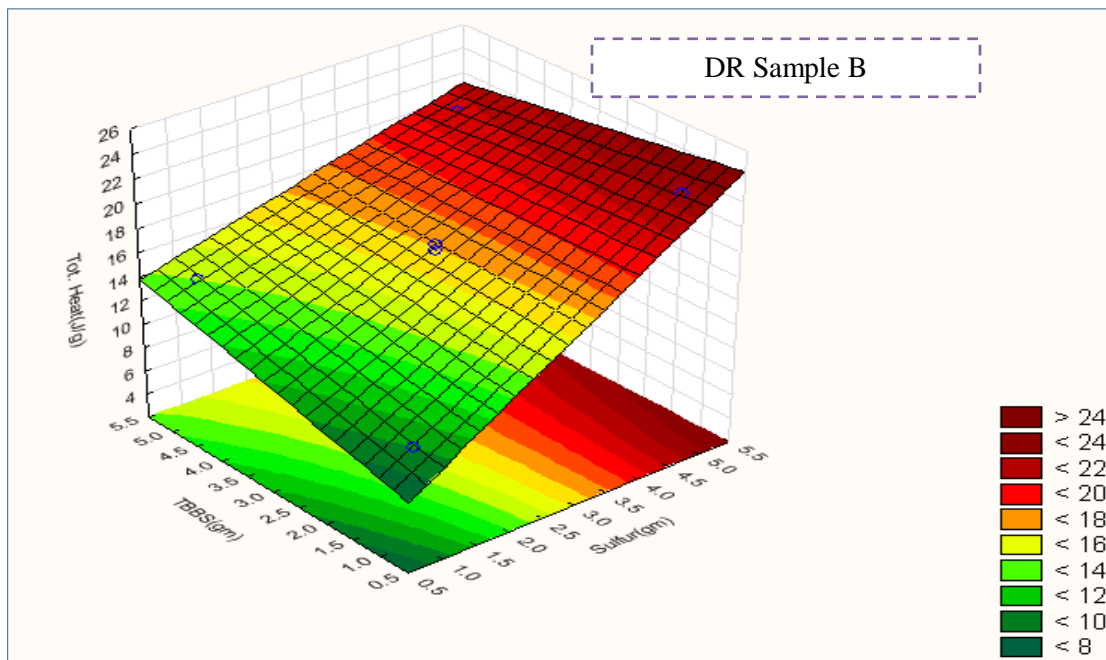


Figure 5.11: Predicted values versus observed values.

Comparison of total heat of reaction between NR and DR





**Figure 5.12: Effect of change in curative composition in total heat of reaction for NR and DR.**

To compare the heat of reaction data for both NR and DR a three dimensional graphs (Figure 5.12) showing the effect of change in curative composition (sulphur and accelerators) on total heat of reaction was generated using Statistica. These graphs show that NR and DR follow similar trends for total heat of reaction with change in curative composition, but the magnitude of heat is less in the case of DR compared to NR. This could be a result of lower amount of double bonds available in case of DR to form cross links and thus resulting in low heat of reaction.

### 5.1.3 Model Fitting

Data obtained from DSC scans at 5, 10, 15, 20 and 25 °C/min were used to first determine the activation energy (E1) using the Kissinger and Arrhenius models. Also, the heat data were used to calculate the degree of cure (c) and reaction rate (dc/dt). Later this information was given as an input (E1, dc/dt, c, time, temperature, initial guess matrix) to the software to estimate the parameters (Table 5.9 and 5.10) in the Kamal-Sourour model. It was seen that the estimated dc/dt and c data were in good agreement with the experimental data for both NR and DR samples. Representative results for some samples are shown in Figures 5.13 and 5.15. In order to validate the estimated parameters the model was used to predict data for dc/dt and c at a scan rate (15°C/min for NR and 15°C/min for DR) that was not used for fitting and it was seen that the predicted data are comparable to the experimental data (Figures 5.14 and 5.16).

The estimated constants for the model parameters (shown in eq. 4.11) obtained for both NR sample B and DR sample after fitting the model to DSC data are shown in Table 5.9 and Table 5.10.

**Table 5.9: Estimated constants for NR sample B.**

<b>Parameter</b>	<b>a<sub>i1</sub></b>	<b>a<sub>i2</sub></b>	<b>a<sub>i3</sub></b>
<b>m</b>	<b>55.92</b>	<b>-0.20</b>	<b>1.65E-04</b>
<b>n</b>	<b>-1.61</b>	<b>1.920</b>	<b>-2.78E-05</b>
<b>a1</b>	<b>5.76</b>	<b>-2.7E-02</b>	<b>3.2E-05</b>
<b>a2</b>	<b>-1.25E-02</b>	<b>5.6E-05</b>	<b>-6.16E-08</b>
<b>E2</b>	<b>-11362.14</b>	<b>0</b>	<b>0</b>
<b>E1</b>	<b>9249.05</b>	<b>0</b>	<b>0</b>

**Table 5.10: Estimated constants for DR sample B.**

Parameter	$a_{i1}$	$a_{i2}$	$a_{i3}$
<b>m</b>	<b>36.21</b>	<b>-0.12</b>	<b>7.77E-05</b>
<b>n</b>	<b>44.44</b>	<b>-0.15</b>	<b>1.38E-04</b>
<b>a1</b>	<b>4.64</b>	<b>-2.21E-02</b>	<b>2.63E-05</b>
<b>a2</b>	<b>-1.34E-02</b>	<b>5.39E-05</b>	<b>-6.27E-08</b>
<b>E2</b>	<b>563.66</b>	<b>0</b>	<b>0</b>
<b>E1</b>	<b>2639.94</b>	<b>0</b>	<b>0</b>

Once these parameters are estimated, reaction rate ( $dc/dt$ ) data was predicted using those constants to have a comparison with the experimental data for both NR and DR samples. A graph showing the  $dc/dt$  values for predicted and experimental data for each rubber samples were plotted to see if the predicted values are in agreement with the experimental data (Figure 5.13 and Figure 5.15).

- **For NR samples:** Scan rates used to estimate the parameters: 5, 10 and 20°C/min.

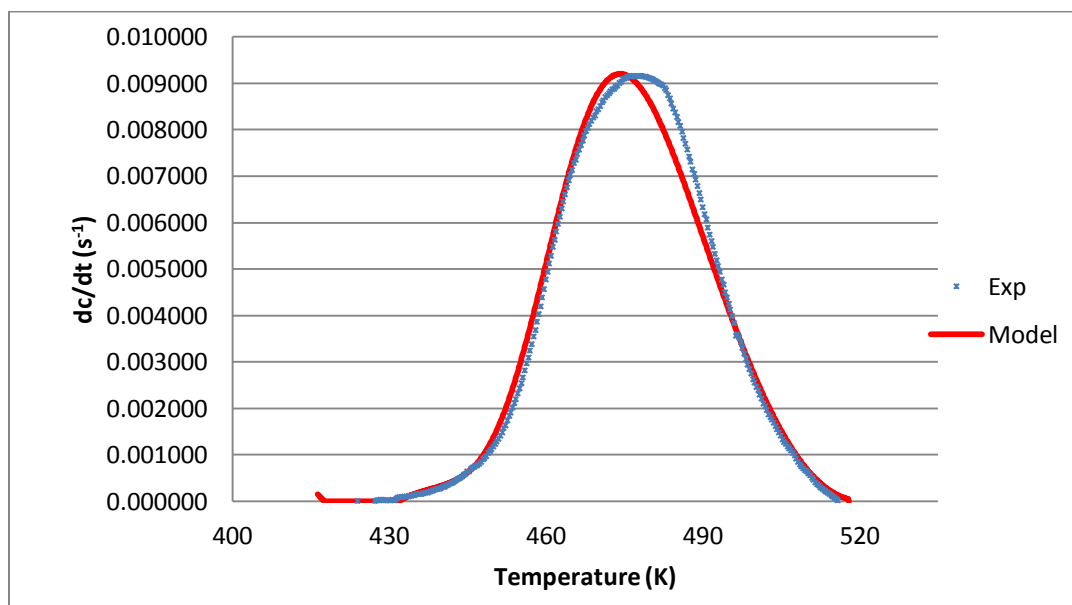


**Figure 5.13: Fitted model vs. experimental data for NR sample B at 20°C/min.**

In order to validate the model, the estimated parameters were later used to predict the reaction rate ( $dc/dt$ ) for the scan rate  $15^{\circ}\text{C}/\text{min}$  (which was not used for parameter estimation). Finally, the predicted  $dc/dt$  data were compared with experimental data (Figure 5.13).

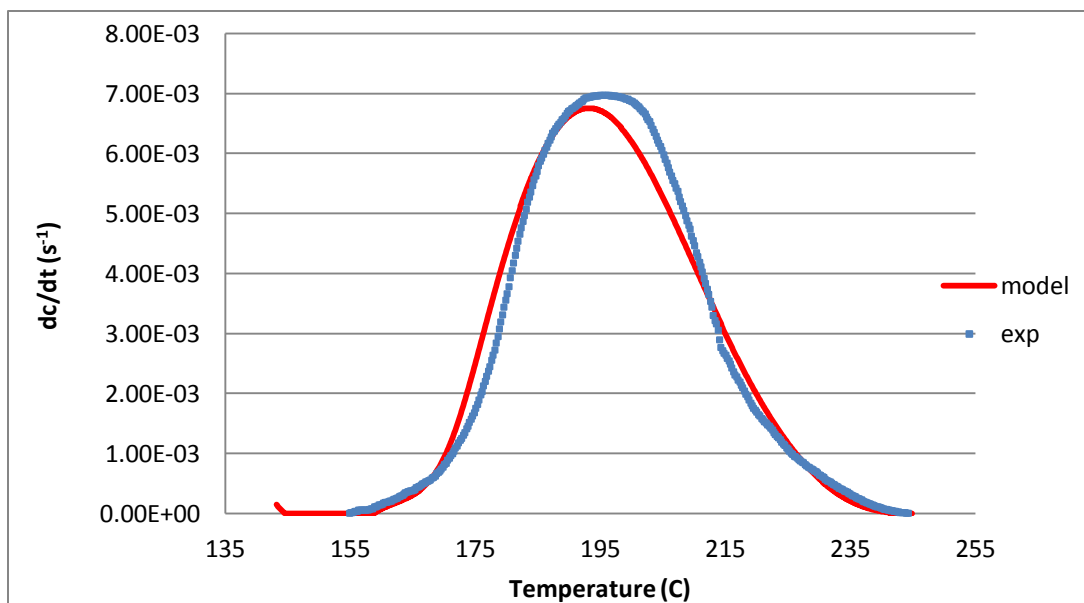


**Figure 5.14: Predicted data vs experimental data for NR sample B at  $15^{\circ}\text{C}/\text{min}$ .**

- **For DR samples:** Scan rates used to determine the constants:  $10$ ,  $15$  and  $25^{\circ}\text{C}/\text{min}$ .

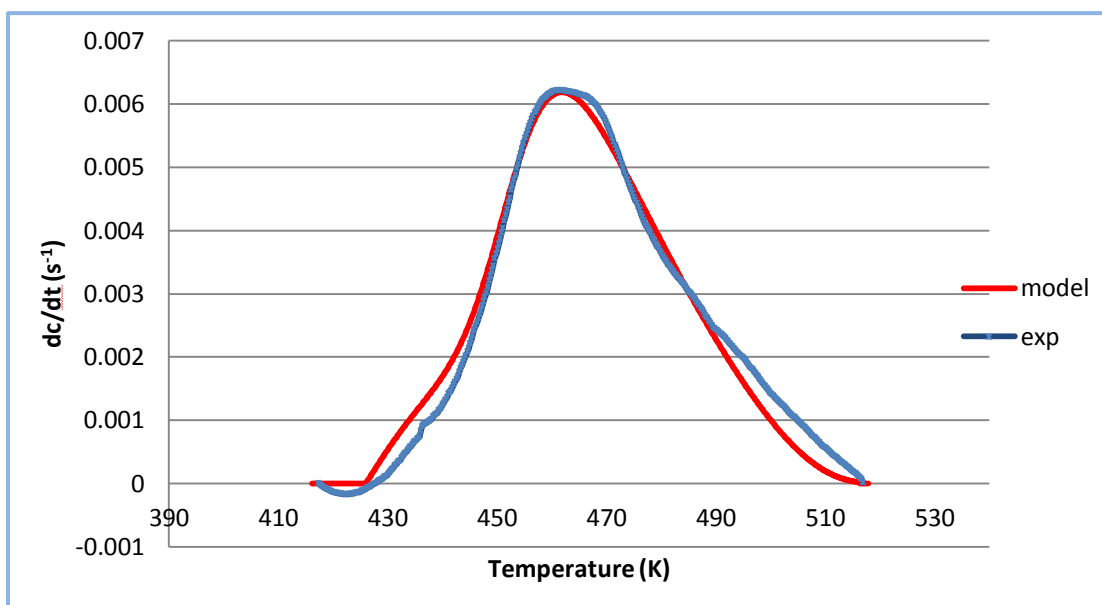


**Figure 5.15: Fitted model vs. experimental data for DR sample B at  $15^{\circ}\text{C}/\text{min}$ .**

In order to validate the model for DR sample B, the estimated parameters determined by using the model were later used to predict the reaction rate ( $dc/dt$ ) for the scan rate  $20^{\circ}\text{C}/\text{min}$  (which was not used for parameter estimation). Finally the predicted  $dc/dt$  data was compared with experimental data (Figure 5.16).

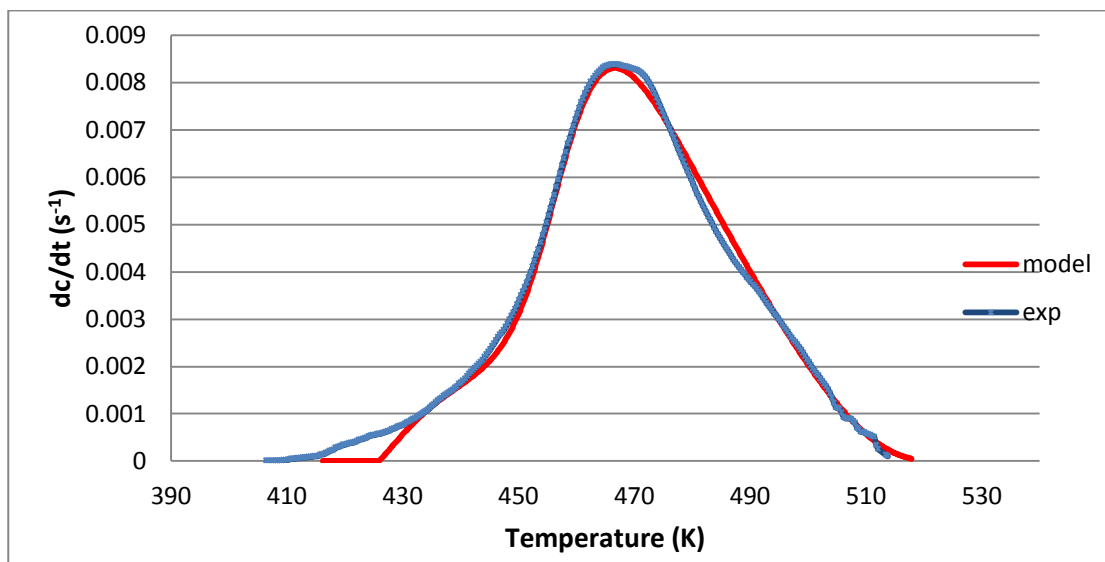


**Figure 5.16: Predicted data vs experimental data for DR sample B at  $20^{\circ}\text{C}/\text{min}$ .**

## 5.2 Master Batch Compound and Blends

To test the ability of the model to predict curing behavior for DR-blends, three blends with 10%, 20% and 30% of DR with a virgin rubber (master batch of Tire tread compound/ MB) was tested along with a sample of only the master batch compound.

### 5.2.1 DSC

MB compound and MB-DR blend samples were scanned using DSC at different scan rates. The heat of reaction and peak temperature for each sample was calculated and shown in Table 5.11 - Table 5.14.

**Table 5.11:  $T_{\text{peak}}$  and total heat of reaction for the MB compound.**

Scan Rate ( $^{\circ}\text{C}/\text{min}$ )	Sample mass (mg)	$T_{\text{peak}}$ ( $^{\circ}\text{C}$ )	Total heat of reaction (J/g)
5	7.2	177.7	29.4
10	7.3	191.8	27.0
15	8.32	198.4	30.7
20	7.74	203.9	24.6
25	8.23	208.9	21.6
35	8.26	213.5	26.9
40	7.75	216.6	25.9

**Table 5.12:  $T_{\text{peak}}$  and heat of reaction for MB/DR20 blends.**

Scan Rate ( $^{\circ}\text{C}/\text{min}$ )	Sample mass (mg)	$T_{\text{peak}}$ ( $^{\circ}\text{C}$ )	Total heat of reaction (J/g)
5	7.55	174.6	21.1
10	7.53	187.4	23.9
15	7.13	195.1	25.7
20	7.64	201.1	25.3
25	8.51	205.3	22.1
30	7.67	210.7	24.5
40	7.2	216.1	24.7

**Table 5.13: T<sub>peak</sub> and heat of reaction for MB/DR10 blends.**

Scan Rate (°C/min)	Sample mass (mg)	T <sub>peak</sub> (°C)	Total heat of reaction (J/g)
10	8.01	198.1	15.8
15	7.60	199.5	17.3
20	7.72	203.3	17.4
25	8.70	207.5	15.7
30	8.43	211.6	16.5
35	8.75	212.0	16.8

**Table 5.14: T<sub>peak</sub> and heat of reaction for MB/DR30 blends.**

Scan Rate (°C/min)	Sample mass (mg)	T <sub>peak</sub> (°C)	Total heat of reaction (J/g)
10	7.01	189.8	15.3
15	8.17	194.6	17.4
20	7.49	199.1	14.6
25	7.83	204.3	16.1
30	8.07	206.6	15.6
35	8.10	211.5	20.3

### 5.2.2 Model Fitting

After the heat data was calculated from DSC results, peak temperature and heating rates were used to calculate activation energy and also  $dc/dt$  and  $c$  was calculated from the DSC data. Later these data were given as an input to the program with initial guess matrix to fit the model and estimate the parameters. The estimated parameters for the MB samples and DR/MB samples are shown in Tables 5.15- 5.18. Once these parameters are estimated, reaction rate ( $dc/dt$ ) data was predicted using those constants to have a comparison with the experimental data for all the samples.

Also plots for fitted model and experimental data are shown in Figures 5.17 to see if the predicted values are in agreement with the experimental data.

- **MB compound:** Scan rates used to determine the constants: 5, 10, 15, 20, 25, and 30°C/min.

**Table 5.15: Estimated constants for MB.**

Parameter	$a_{i1}$	$a_{i2}$	$a_{i3}$
<b>m</b>	<b>-0.84</b>	<b>3.55</b>	<b>-6.67E-05</b>
<b>n</b>	<b>109.78</b>	<b>-0.42</b>	<b>3.97E-04</b>
<b>a1</b>	<b>0.44</b>	<b>-2.11E-03</b>	<b>2.54E-06</b>
<b>a2</b>	<b>-3.31</b>	<b>1.49E-02</b>	<b>-1.64E-05</b>
<b>E2</b>	<b>1980.22</b>	<b>0</b>	<b>0</b>
<b>E1</b>	<b>15844.11</b>	<b>0</b>	<b>0</b>

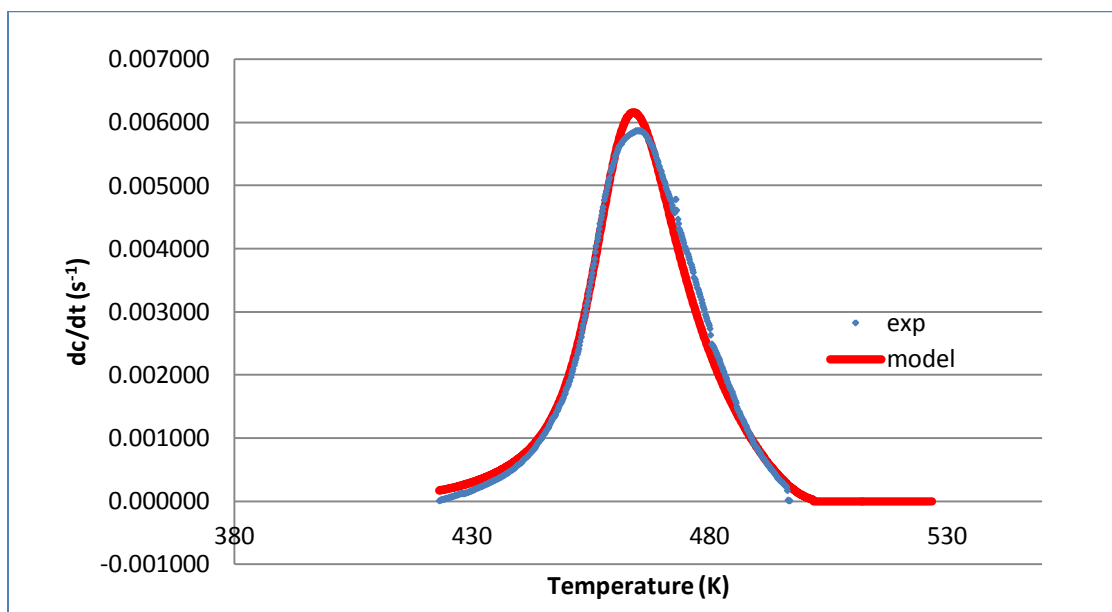


**Figure 5.17: Fitted model vs experimental data for MB sample at 10°C/min.**

In order to validate the model, the estimated parameters determined by using the model were later used to predict the reaction rate ( $dc/dt$ ) for the scan rate  $40^{\circ}\text{C}/\text{min}$  (which was not used for parameter estimation). Finally the predicted  $dc/dt$  data was compared with experimental data (Figure 5.18).

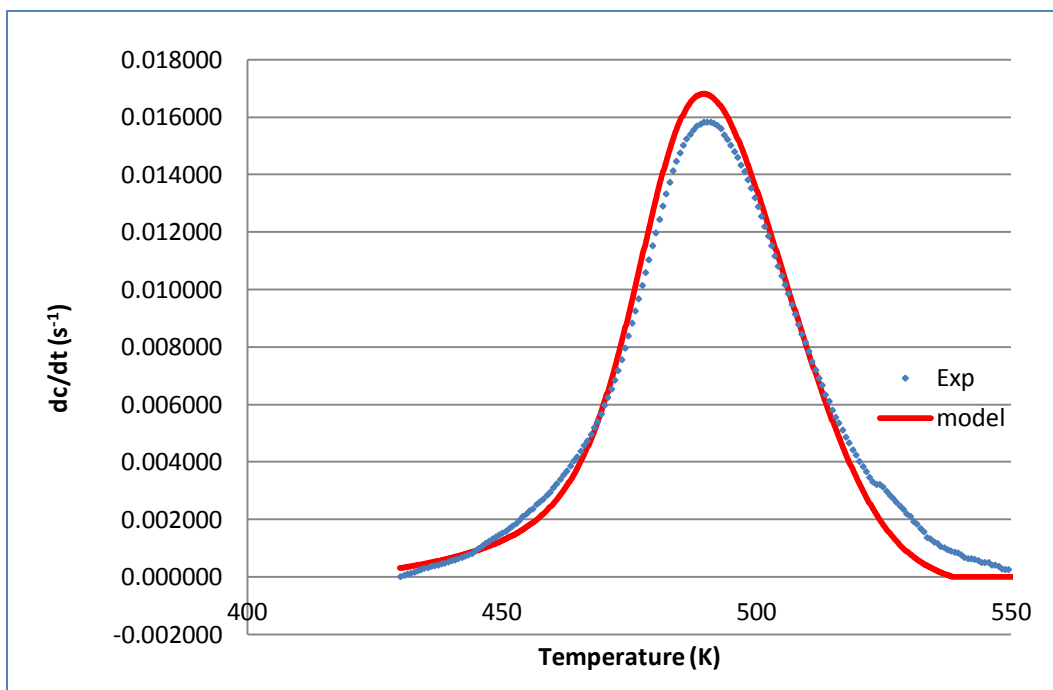


**Figure 5.18: Predicted data vs experimental data for MB sample at  $40^{\circ}\text{C}/\text{min}$ .**

➤ **MB/ DR blends**

- **MB/ DR20 blend** Scan rates used to determine the constants: 5, 10, 15, 20, 25 and  $30^{\circ}\text{C}/\text{min}$ .

**Table 5.16: Estimated constants for MB/DR20.**

Parameter	$a_{i1}$	$a_{i2}$	$a_{i3}$
<b>m</b>	<b>21.17</b>	<b>-7.79E-02</b>	<b>7.24E-05</b>
<b>n</b>	<b>23.71</b>	<b>-7.95E-02</b>	<b>6.80E-05</b>
<b>a1</b>	<b>-0.14</b>	<b>6.16E-04</b>	<b>-6.69E-07</b>
<b>a2</b>	<b>-49982.30</b>	<b>216.09</b>	<b>-0.22</b>
<b>E2</b>	<b>41039.83</b>	<b>0</b>	<b>0</b>
<b>E1</b>	<b>12702.06</b>	<b>0</b>	<b>0</b>

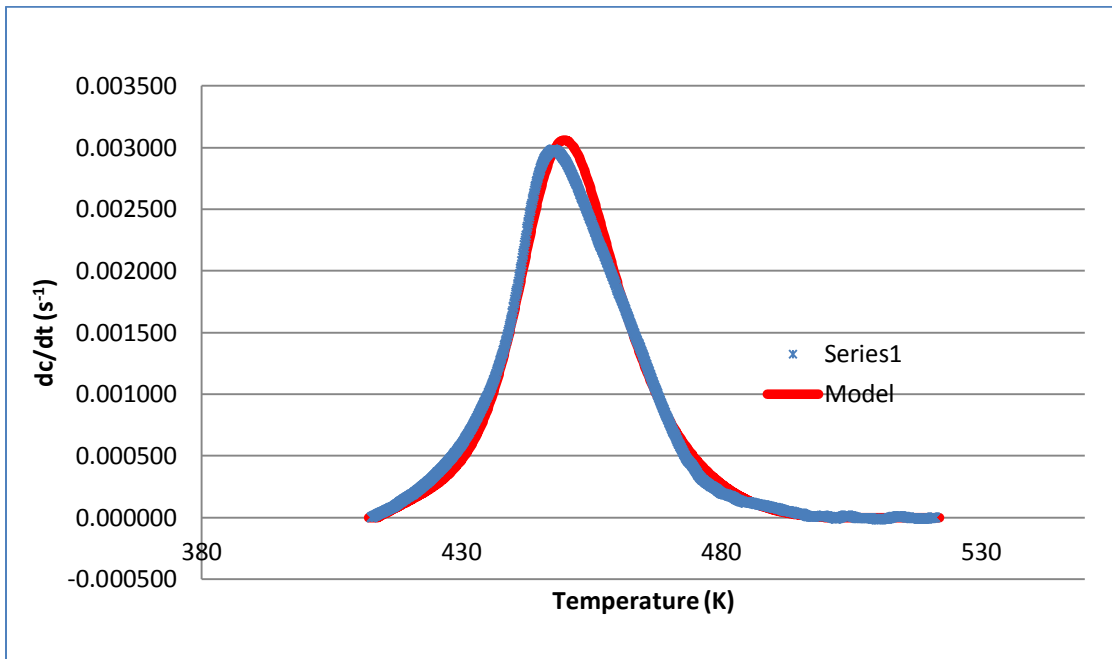


**Figure 5.19: Fitted model vs Experimental data for MB/DR20 sample at 5°C/min.**

In order to validate the model for the blends, the estimated parameters determined by using the model were later used to predict the reaction rate ( $dc/dt$ ) for the scan rate 35°C/min (which was not used for parameter estimation). Finally the predicted  $dc/dt$  data was compared with experimental data (Figure 5.20).

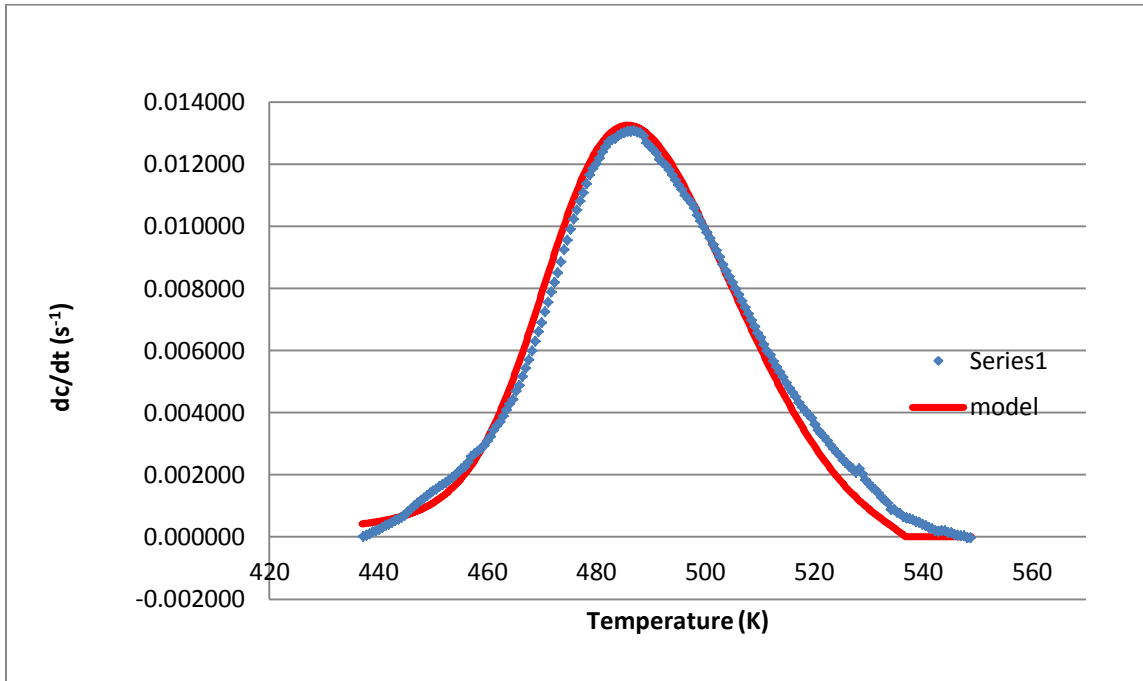


**Figure 5.20: Predicted data vs experimental data for MB/DR20 sample at 35°C/min.**

- **MB/ DR10 blend:** Scan rates used to determine the constants: 10, 15, 20, 25, 30 and 35°C/min.

**Table 5.17: Estimated constants for MB/DR10.**

<b>Parameter</b>	<b>a<sub>i1</sub></b>	<b>a<sub>i2</sub></b>	<b>a<sub>i3</sub></b>
<b>m</b>	<b>157.41</b>	<b>-0.691</b>	<b>7.65E-04</b>
<b>n</b>	<b>215.64</b>	<b>-0.793</b>	<b>7.32E-04</b>
<b>a1</b>	<b>1422.85</b>	<b>-6.284</b>	<b>6.94E-03</b>
<b>a2</b>	<b>54.86</b>	<b>-0.237</b>	<b>2.57E-04</b>
<b>E2</b>	<b>-4460.36</b>	<b>0</b>	<b>0</b>
<b>E1</b>	<b>22909.77</b>	<b>0</b>	<b>0</b>

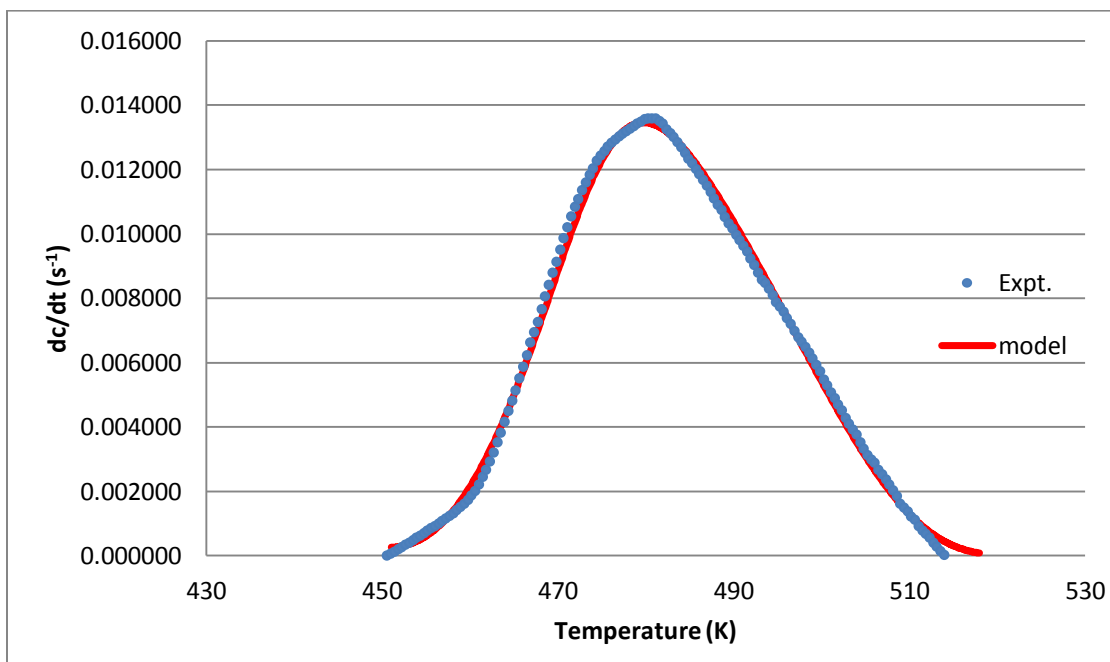


**Figure 5.21: Predicted data vs experimental data for MB/DR10 sample at 25°C/min.**

To validate the model the estimated parameters determined by using the model were used to predict the reaction rate ( $dc/dt$ ) for the scan rates 18 °C/min and compared with experimental data:

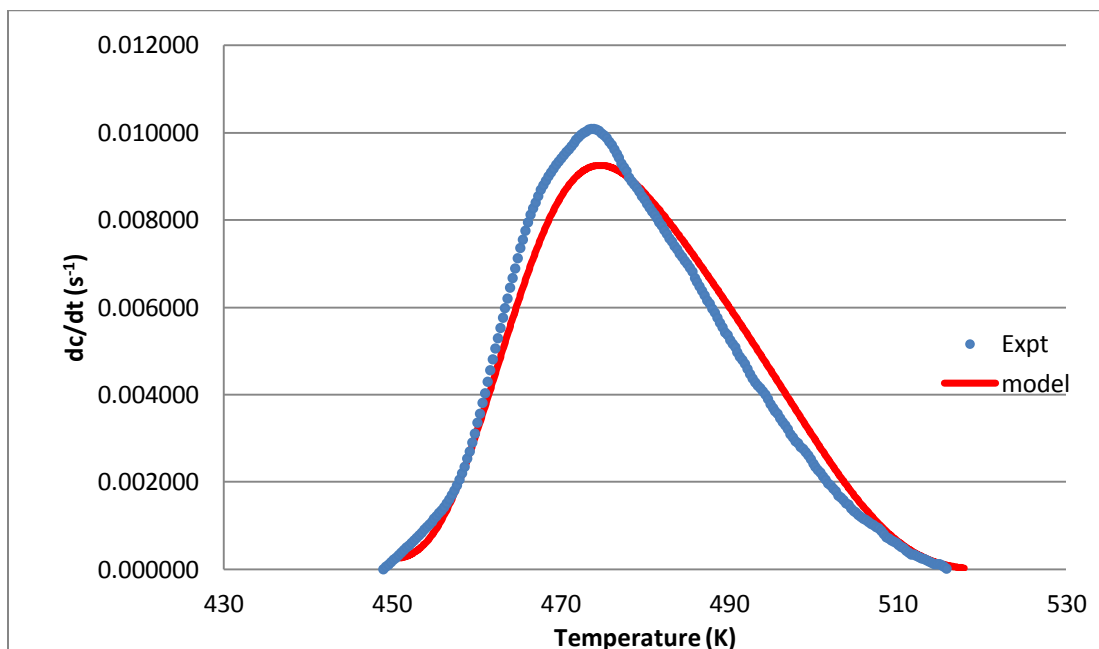


**Figure 5.22: Predicted data vs experimental data for MB/DR10 sample at 18°C/min.**

- **MB/ DR30 blend:** Scan rates used to determine the constants: 10, 15, 20, 25, 30 and 35°C/min.

**Table 5.18: Estimated constants for MB/DR30**

Parameter	$a_{i1}$	$a_{i2}$	$a_{i3}$
<b>m</b>	<b>115.33</b>	<b>-0.49</b>	<b>5.13E-04</b>
<b>n</b>	<b>83.77</b>	<b>-0.32</b>	<b>3.02E-04</b>
<b>a1</b>	<b>-71.12</b>	<b>0.32</b>	<b>-3.51E-04</b>
<b>a2</b>	<b>3.62E-05</b>	<b>-1.62E-07</b>	<b>1.83E-10</b>
<b>E2</b>	<b>-49044.20</b>	<b>0</b>	<b>0</b>
<b>E1</b>	<b>15804.20</b>	<b>0</b>	<b>0</b>

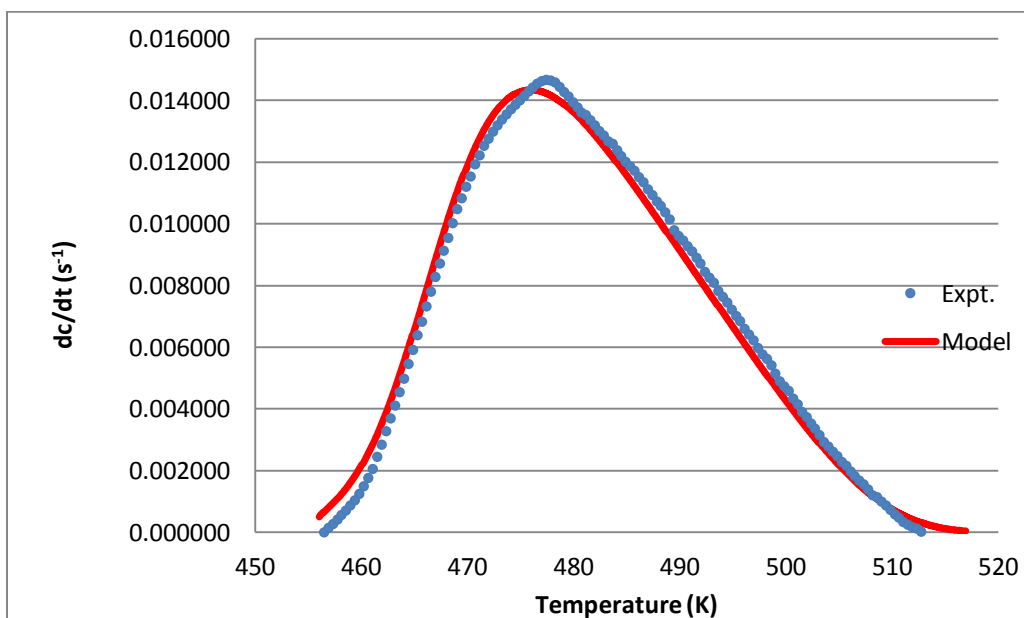


**Figure 5.23: Predicted data vs experimental data for MB/DR30 sample at 25°C/min.**

To validate the model the estimated parameters determined by using the model were used to predict the reaction rate ( $dc/dt$ ) for the scan rates 22.5 °C/min and compared with experimental data:

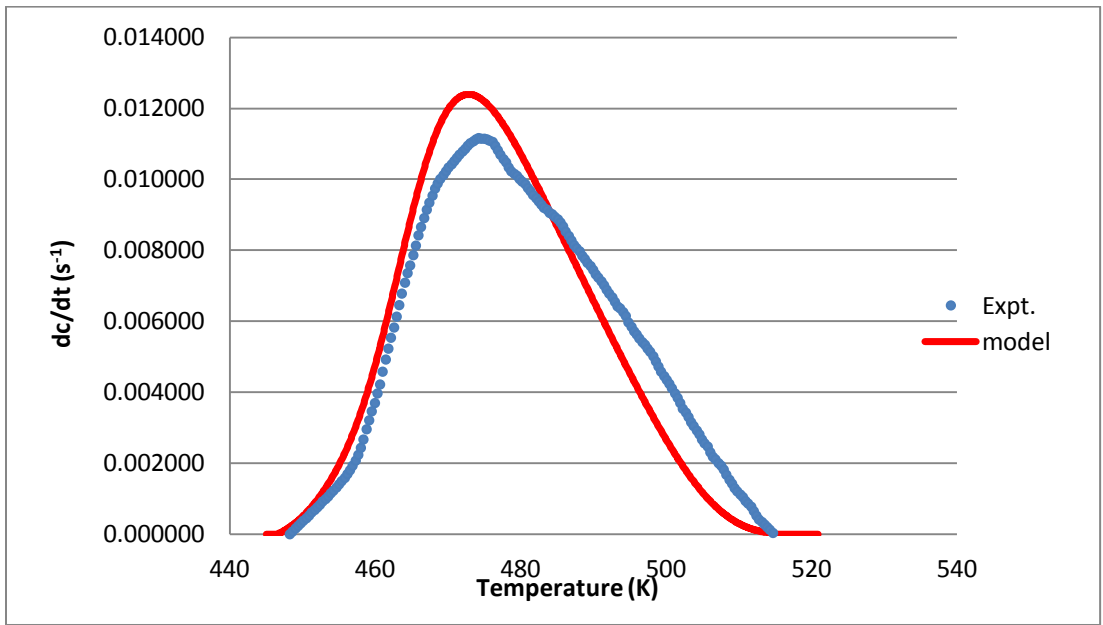


**Figure 5.24: Predicted data vs experimental data for MB/DR30 sample at 22.5°C/min.**

## Chapter 6

### Conclusions and Recommendations

#### Conclusions

The work presented in this thesis addressed the development of a model for the vulcanization reaction of devulcanized rubber. The objectives of the research were:

- To study the effect of some variations in curative composition on the vulcanization reaction of DR and virgin rubber.
- To compare the curing characteristics of DR and virgin rubber via DSC experiments.
- To describe the vulcanization reaction of devulcanized rubber using a kinetic model.

From the experiments conducted and analysis completed, the following observations were made:

- When using different scan rates in DSC, it was observed that an increase in the scan rate led to an increase in peak temperature. This may be due to the pronounced effect of accelerators at faster scan rates.
- The total heat of reaction for a sample at different scan rates was approximately constant, which shows that scan rate does not have a significant effect on the extent of the vulcanization reaction.
- To study the effect of curative composition on vulcanization, the sulfur/accelerator ratio was varied. It was observed that with an increase in accelerator level, the peak temperature (temperature at which the reaction rate is maximum) increased.

The total heat of reaction was observed to be highest when the sulfur dosage was maximum (high Sulfur/Accelerator ratio). However, when the sulfur concentration was kept at the highest level an increase in accelerator dosage resulted in a reduction of the total heat of reaction. This may be due to the

fact that accelerator promotes mono- and di- sulfidic bonds while in non-accelerated sulfur vulcanization more polysulfidic bonds are formed. Also, in non-accelerated sulfur vulcanization there may be some slow side reactions taking place over the long period of vulcanization which can contribute to the total heat of reaction.

➤ It may be worth mentioning that narrower peaks were observed in the DSC curves for the samples containing higher accelerator dosages. This difference in the curing curves has been the result of a different reaction mechanism followed by accelerated sulfur vulcanization, which is predominant in higher accelerated dosage.

➤ It was also observed that addition of accelerator had little effect on the curing behavior of the devulcanized rubber. However, addition of sulfur considerably increased the heat of reaction. This can be seen if we compare samples A, D and B. Similar observations were made by Isayev's group<sup>[23]</sup> while studying the effect of curatives on vulcanization of ultrasonically devulcanized rubber.

➤ From the statistical analysis, it was seen that sulfur has a significant effect on the total heat of reaction. Accelerator concentration and interaction between sulfur and accelerator concentrations become significant only at higher scan rates. This may be due to the reason that at a faster scan rate when the temperature increases quickly, the role of accelerator becomes more prominent.

The total heat of reaction for both NR and DR was compared and it was found that both rubbers follow a similar trend with respect to changes in amount of curatives but the magnitude of total reaction heat is higher for NR compared to DR. This phenomenon can be explained by the fact that sulfur vulcanization requires the presence of unsaturation in the rubber which is higher in the virgin NR.

➤ The activation energy for the curing reaction calculated for devulcanized rubber was seen to be lower than that of the virgin rubber. This indicates that the vulcanization reaction of devulcanized rubber is less affected by temperature.

➤ Model fitting was performed and model parameters were estimated for NR, DR, MB, and MB/DR blends. In order to validate the estimated parameters, predicted data were compared to the experimental data and it was seen that the predicted data were in good agreement with the experimental data.

### **Recommendations**

➤ To gain a better understanding and to support the observations made on the effect of curatives on the total heat of reaction, tests involving determination of the type of bonds present (mono-, di- or poly-sulfidic bonds) should be carried out in future studies.

➤ Also, to study the effect of curatives, the design of experiments in this study accounted only for sulfur and accelerator variation keeping other ingredients concentrations like ZnO and st A. constant. Therefore, more systematic experiments involving the concentrations of ZnO and both ZnO and stA need to be done to fully assess the curing recipe effect on the total heat of reaction. A study by Coran's group<sup>[9, 69]</sup> showed that the presence of ZnO can change the curing mechanism significantly, so the change in dosage of ZnO with respect to the amount of sulfur/accelerator ratio used should be investigated.

➤ More experiments can be carried out to check the model accuracy. Some experiments can also be done by allowing the sample to cure until a certain point and then calculating the degree of cure and crosschecking with the value predicted by the model for curing up to that particular time.

➤ Finally, due to the small sample amount used in DSC, inhomogeneities in the DR material may affect the results obtained. Future curing experiments should be conducted using an oscillatory disk rheometer (ODR). ODR uses a larger sample and in addition can detect reversion which is not accounted for in DSC.

## Appendix A

### DSC Results for NR Samples

**Table A.1: Scans at Heating Rate 5 °C/min**

<b>Sample</b>	<b>Sample mass (mg)</b>	<b>Tpeak (°C)</b>	<b>Total heat of reaction (J/g)</b>
<b>A</b>	<b>7.2</b>	178.3	2.1
<b>B</b>	<b>7.24</b>	172.3	24.5
<b>C1</b>	<b>7.24</b>	175.5	17.2
<b>C2</b>	<b>7.26</b>	175.5	7.2
<b>C3</b>	<b>7.26</b>	174.7	15.5
<b>D</b>	<b>7.2</b>	182.2	4.9
<b>E</b>	<b>7.18</b>	172.1	20.3

**Table A.2: Scans at Heating Rate 10 °C/min**

<b>Sample</b>	<b>Sample mass (mg)</b>	<b>Tpeak (°C)</b>	<b>Total heat of reaction ( J/g)</b>
<b>A</b>	<b>7.21</b>	192.4	11.8
<b>B</b>	<b>7.05</b>	183.5	31.6
<b>C1</b>	<b>7.18</b>	186.2	19.0
<b>C2</b>	<b>7.26</b>	186.2	19.0
<b>C3</b>	<b>7.12</b>	186.2	19.1
<b>D</b>	<b>7.04</b>	194.7	12.0
<b>E</b>	<b>7.09</b>	183.4	27.2

**Table A.3: Scans at Heating Rate 15 °C/min.**

<b>Sample</b>	<b>Sample mass (mg)</b>	<b>T<sub>peak</sub> (°C)</b>	<b>Total heat of reaction (J/g)</b>
<b>A</b>	<b>7.16</b>	199.7	12.8
<b>B</b>	<b>7.1</b>	195.0	31.1
<b>C1</b>	<b>7.19</b>	193.8	19.6
<b>C2</b>	<b>7.18</b>	192.4	19.9
<b>C3</b>	<b>7.16</b>	193.1	19.9
<b>D</b>	<b>7.21</b>	200.6	12.3
<b>E</b>	<b>7.23</b>	191.1	25.9

**DSC Results for DR Samples**

**Table A.4: Scans at Heating Rate 15 °C/min**

<b>Sample</b>	<b>Sample mass (mg)</b>	<b>T<sub>peak</sub> (°C)</b>	<b>Total heat of reaction (J/g)</b>
<b>A</b>	<b>7.13</b>	189.9	14.1
<b>B</b>	<b>7.12</b>	187.9	31.1
<b>C1</b>	<b>7.17</b>	183.7	26.3
<b>C2</b>	<b>7.12</b>	184.4	21.4
<b>C3</b>	<b>7.15</b>	183.4	24.2
<b>D</b>	<b>7.15</b>	183.6	19.2
<b>E</b>	<b>7.11</b>	181.8	26.5

**Table A.5: Scans at Heating Rate 25 °C/min**

<b>Sample</b>	<b>Sample mass (mg)</b>	<b>T<sub>peak</sub> (°C)</b>	<b>Total heat of reaction (J/g)</b>
<b>A</b>	<b>7.15</b>	201.8	15.3
<b>B</b>	<b>7.12</b>	199.4	30.7
<b>C1</b>	<b>7.20</b>	194.6	26.2
<b>C2</b>	<b>7.27</b>	194.3	25.3
<b>C3</b>	<b>7.18</b>	194.2	24.2
<b>D</b>	<b>7.17</b>	194.7	19.1
<b>E</b>	<b>7.10</b>	192.6	26.5

**Estimated Parameters:**

**Table A.6: Estimated constants for NR Sample A.**

<b>Parameter</b>	<b>a<sub>i1</sub></b>	<b>a<sub>i2</sub></b>	<b>a<sub>i3</sub></b>
<b>m</b>	<b>-431.47</b>	<b>1.92</b>	<b>-2.13E-03</b>
<b>n</b>	<b>160.34</b>	<b>-0.68</b>	<b>7.23E-04</b>
<b>a1</b>	<b>-142.48</b>	<b>0.625</b>	<b>-6.86E-04</b>
<b>a2</b>	<b>168835.89</b>	<b>-713.34</b>	<b>0.75</b>
<b>E2</b>	<b>37630.78</b>	<b>0</b>	<b>0</b>
<b>E1</b>	<b>13164.35</b>	<b>0</b>	<b>0</b>

**Table A.7: Estimated constants for NR Sample C.**

<b>Parameter</b>	<b>a<sub>i1</sub></b>	<b>a<sub>i2</sub></b>	<b>a<sub>i3</sub></b>
<b>m</b>	<b>-562.84</b>	<b>2.50</b>	<b>-2.78E-03</b>
<b>n</b>	<b>693.92</b>	<b>-2.85</b>	<b>2.93E-03</b>
<b>a1</b>	<b>-24.00</b>	<b>0.10</b>	<b>-1.13E-04</b>
<b>a2</b>	<b>2.41E-06</b>	<b>-9.96E-09</b>	<b>1.03E-11</b>
<b>E2</b>	<b>-64294.68</b>	<b>0</b>	<b>0</b>
<b>E1</b>	<b>14207.82</b>	<b>0</b>	<b>0</b>

**Table A.8: Estimated constants for NR Sample D.**

<b>Parameter</b>	<b>a<sub>i1</sub></b>	<b>a<sub>i2</sub></b>	<b>a<sub>i3</sub></b>
<b>m</b>	<b>578.20</b>	<b>-2.44</b>	<b>2.57E-03</b>
<b>n</b>	<b>-232.72</b>	<b>0.971</b>	<b>-1.01E-03</b>
<b>a1</b>	<b>-237.53</b>	<b>1.04</b>	<b>-1.14E-03</b>
<b>a2</b>	<b>-6908.39</b>	<b>28.48</b>	<b>-2.92E-02</b>
<b>E2</b>	<b>24692.27</b>	<b>0</b>	<b>0</b>
<b>E1</b>	<b>15338.59</b>	<b>0</b>	<b>0</b>

**Table A.9: Estimated constants for NR Sample E.**

<b>Parameter</b>	<b>a<sub>i1</sub></b>	<b>a<sub>i2</sub></b>	<b>a<sub>i3</sub></b>
<b>m</b>	<b>-467.94</b>	<b>2.09</b>	<b>-2.34E-03</b>
<b>n</b>	<b>1491.29</b>	<b>-6.17</b>	<b>6.39E-03</b>
<b>a1</b>	<b>9.91</b>	<b>-4.61E-02</b>	<b>5.36E-05</b>
<b>a2</b>	<b>1.66E-09</b>	<b>-6.89E-12</b>	<b>7.15E-15</b>
<b>E2</b>	<b>-98216.84</b>	<b>0</b>	<b>0</b>
<b>E1</b>	<b>13139.40</b>	<b>0</b>	<b>0</b>

**Table A.10: Estimated constants for DR Sample A.**

<b>Parameter</b>	<b>a<sub>i1</sub></b>	<b>a<sub>i2</sub></b>	<b>a<sub>i3</sub></b>
<b>m</b>	<b>399.98</b>	<b>-1.74</b>	<b>1.90E-03</b>
<b>n</b>	<b>158.85</b>	<b>-0.65</b>	<b>6.74E-04</b>
<b>a1</b>	<b>-15.56</b>	<b>7.13E-02</b>	<b>-8.15E-05</b>
<b>a2</b>	<b>1.93E-04</b>	<b>-8.61E-07</b>	<b>9.61E-10</b>
<b>E2</b>	<b>-44724.56</b>	<b>0</b>	<b>0</b>
<b>E1</b>	<b>10530.31</b>	<b>0</b>	<b>0</b>

**Table A.11: Estimated constants for DR Sample C.**

<b>Parameter</b>	<b>a<sub>i1</sub></b>	<b>a<sub>i2</sub></b>	<b>a<sub>i3</sub></b>
<b>m</b>	<b>-417.76</b>	<b>1.88</b>	<b>-2.12E-03</b>
<b>n</b>	<b>-303.33</b>	<b>1.26</b>	<b>-1.30E-03</b>
<b>a1</b>	<b>-51.85</b>	<b>0.23</b>	<b>-2.61E-04</b>
<b>a2</b>	<b>2.74E+11</b>	<b>-1.2E+09</b>	<b>1.23E+06</b>
<b>E2</b>	<b>93069.60</b>	<b>0</b>	<b>0</b>
<b>E1</b>	<b>10586.02</b>	<b>0</b>	<b>0</b>

**Table A.12: Estimated constants for DR Sample D.**

<b>Parameter</b>	<b>a<sub>i1</sub></b>	<b>a<sub>i2</sub></b>	<b>a<sub>i3</sub></b>
<b>m</b>	<b>-890.04</b>	<b>3.97</b>	<b>-4.41E-03</b>
<b>n</b>	<b>223.48</b>	<b>-0.90</b>	<b>9.17E-04</b>
<b>a1</b>	<b>-40.22</b>	<b>0.17</b>	<b>-1.96E-04</b>
<b>a2</b>	<b>1.01E-02</b>	<b>-4.23E-05</b>	<b>4.43E-08</b>
<b>E2</b>	<b>-29340.01</b>	<b>0</b>	<b>0</b>
<b>E1</b>	<b>10450.49</b>	<b>0</b>	<b>0</b>

**Table A.13: Estimated constants for DR Sample E.**

<b>Parameter</b>	<b>a<sub>i1</sub></b>	<b>a<sub>i2</sub></b>	<b>a<sub>i3</sub></b>
<b>m</b>	<b>-386.41</b>	<b>1.59</b>	<b>-1.63E-03</b>
<b>n</b>	<b>46.88</b>	<b>-9.65E-02</b>	<b>1.22E-05</b>
<b>a1</b>	<b>160.76</b>	<b>-0.72</b>	<b>8.09E-04</b>
<b>a2</b>	<b>7.48E+06</b>	<b>-3.37E+04</b>	<b>38.01</b>
<b>E2</b>	<b>34295.89</b>	<b>0</b>	<b>0</b>
<b>E1</b>	<b>10615.12</b>	<b>0</b>	<b>0</b>

## Bibliography

- [1] Avraam, A.I. (2005). Recycling of rubber. In J.E. Mark, B. Erman, and M. Roland (Eds.), *The Science and Technology of Rubber* (pp.663-695). Amsterdam: Academic Press.
- [2] Morton, M. (1987). Rubber technology. *Van Nostrand Reinhold Company Co, Molly Millars Lane, Wokingham, Berkshire RG 11 2 PY, UK*, 1987.
- [3] Gowariker, V. R., Viswanathan, N. V., and Sreedhar, J. (1986). *Polymer Science*. New Age International.
- [4] Hills, D. A. (1971). *Heat Transfer and Vulcanisation of Rubber*. Elsevier Publishing Company, Essex, England.
- [5] Alliger, G., and Sjothun, I. J. (Eds.). (1964). *Vulcanization of Elastomers: principles and practice of vulcanization of commercial rubbers*. Reinhold Pub. Corp.
- [6] Blow, C. M., and Hepburn, C. (1982). *Rubber Technology and Manufacture*. Oxford, UK: Butterworth-Heinemann Ltd.
- [7] Mark, J. E., Erman, B., and Roland, M. (Eds.). (2005). *The Science and Technology of Rubber*. Amsterdam: Academic Press.
- [8] Datta, R. N., and Flexsys, B. V. (2002). *Rubber Curing Systems*. Rapra Technology Limited.
- [9] Coran, A.Y. (2005). Vulcanization. In J.E. Mark, B. Erman, and M. Roland (Eds.), *The Science and Technology of Rubber* (pp.321-361). Amsterdam: Academic Press.
- [10] Clark, C., Meardon, K., and Russell, D. (1993). *Scrap tire technology and markets* (No. 211). Park Ridge,N.J., U.S.A. : Noyes Data Corporation.
- [11] Rubber Manufacturers Association. (2009).Scrap tire markets in the United States. *9th biennial report*.

- [12] Rubber Manufacturers Association. (2013). 2011 U.S. scrap tire market summary. Washington, DC, U.S.A.
- [13] Adhikari, B., De, D., and Maiti, S. (2000). *Reclamation and Recycling of Waste Rubber*. *Progress in Polymer Science*, 25(7), 909-948.
- [14] Sutanto, P(2006). *Development of a Continuous Process for EPDM Devulcanization in an Extruder*. PhD Dissertation, University of Twente, Netherlands.
- [15] Maxwell, B. (1979). *U.S. Patent No. 4,146,508*. Washington, DC: U.S. Patent and Trademark Office.
- [16] Cerny, G. L., and Keith A. T. (1984). *U.S. Patent No. 4,459,450*. Washington, DC: U.S. Patent and Trademark Office.
- [17] Clifford, M. L. (1978). *U.S. Patent No. 4,130,616*. Washington, DC: U.S. Patent and Trademark Office.
- [18] Hirayama, D., and Saron, C. (2012). Chemical Modifications in Styrene–Butadiene Rubber after Microwave Devulcanization. *Industrial and Engineering Chemistry Research*, 51(10), 3975-3980.
- [19] Pelofsky, A. H. (1973). *U.S. Patent No. 3,725,314*. Washington, DC: U.S. Patent and Trademark Office.
- [20] Okuda, M., and Y. Hatano. *Method of Desulfurizing Rubber by Ultrasonic Wave*. Japan, 62121741.
- [21] Isayev, A. (1993). *U.S. Patent No. 5,258,413*. Washington, DC: U.S. Patent and Trademark Office.

- [22] Levin, V. Y., Kim, S. H., and Isayev, A. I. (1997). Effect of crosslink type on the ultrasound devulcanization of SBR vulcanizates. *Rubber chemistry and Technology*, 70(4), 641-649.
- [23] Levin, V. Y., Kim, S. H., and Isayev, A. I. (1997). Vulcanization of ultrasonically devulcanized SBR elastomers. *Rubber Chemistry and Technology*, 70(1), 120-128.
- [24] Yun, J., Yashin, V. V., and Isayev, A. I. (2004). Ultrasonic devulcanization of carbon black-filled ethylene propylene diene monomer rubber. *Journal of Applied Polymer Science*, 91(3), 1646-1656.
- [25] Myhre, M., and MacKillop, D. A. (2002). Rubber recycling. *Rubber Chemistry and Technology*, 75(3), 429-474.
- [26] Meysami, M. (2012). *A Study of Scrap Rubber Devulcanization and Incorporation of Devulcanized Rubber into Virgin Rubber Compounds*. Doctoral dissertation, University of Waterloo.
- [27] Fukumori, K., Matsushita, M., Okamoto, H., Sato, N., Suzuki, Y., and Takeuchi, K. (2002). Recycling technology of tire rubber. *JSAE review*, 23(2), 259-264.
- [28] Fukumori, K., Matsushita, M., Mouri, M., Okamoto, H., Sato, N., Takeuchi, K., and Suzuki, Y. (2006). Dynamic devulcanization and dynamic vulcanization for recycling of crosslinked rubber. *KGK. Kautschuk, Gummi, Kunststoffe*, 59(7-8), 405-411.
- [29] Mouri, M., Sato, N., Okamoto, H., Matsushita, M., Hondo, H., Nakashima, K., Takeuchi, K., Suzuki, Y., and Owaki, M. (2000). *A new devulcanization process. Continuous reclamation of rubber by shear flow reaction control technology (Part I)*. *Int. Pol. Sci. and Tech.*, (vol. 27, No. 1, pp. T/17-T/22).

- [30] Mouri, M., Sato, N., Okamoto, H., Matsushita, M., Hondo, H., Nakashima, K., Takeushi, K., Suzuki, Y., and Owaki, M. (2000). *De-vulcanization conditions and mechanical properties of re-vulcanized rubber for EPDM. Continuous reclamation of rubber by shear flow reaction control technology (Part II)*. Int. Pol. Sci. and Tech., (vol. 27, No. 1, pp. T/23-T/28).
- [31] Mouri, M., Sato, N., Okamoto, H., Matsushita, M., Hondo, H., Nakashima, K., Takeushi, K., Suzuki, Y., and Owaki, M. (2000). *Continuous devulcanization by shear flow stage reaction control technology for rubber recycling. Part III. Study of the devulcanization process for EPDM*. Int. Pol. Sci. and Tech., (vol. 27, No. 2, pp. T/12-T/16).
- [32] Mouri, M., Sato, N., Okamoto, H., Matsushita, M., Hondo, H., Nakashima, K., Takeushi, K., Suzuki, Y., and Owaki, M. (2000). *Continuous devulcanization by shear flow stage reaction control technology for rubber recycling. Part IV. Devulcanization mechanism for EPDM*. Int. Pol. Sci. and Tech., (vol. 27, No. 2, pp. T/17-T/22).
- [33] Maridass, B., and Gupta, B. R. (2006). Effect of Carbon Black on Devulcanized Ground Rubber Tire--Natural Rubber Vulcanizates: Cure Characteristics and Mechanical Properties. *Journal of Elastomers and Plastics*, 38(3), 211–229.
- [34] Maridass, B., and Gupta, B. R. (2004). Performance optimization of a counter rotating twin screw extruder for recycling natural rubber vulcanizates using response surface methodology. *Polymer Testing*, 23(4), 377–385.
- [35] Balasubramanian, M. (2008). Cure modeling and mechanical properties of counter rotating twin screw extruder devulcanized ground rubber tire—natural rubber blends. *Journal of Polymer Research*, 16(2), 133–141.

- [36] Sutanto, P., Picchioni, F., and Janssen, L. P. B. M. (2006). The use of experimental design to study the responses of continuous devulcanization processes. *Journal of Applied Polymer Science*, 102(5), 5028–5038.
- [37] Yazdani, H., Karrabi, M., Ghasmi, I., Azizi, H., and Bakhshandeh, G. R. (2011). Devulcanization of Waste Tires Using a Twin-Screw Extruder: The Effects of Processing Conditions.
- [38] Yazdani, H., Ghasemi, I., Karrabi, M., Azizi, H., and Bakhshandeh, G. R. (2013). Continuous Devulcanization of Waste Tires by Using a Co-Rotating Twin Screw Extruder: Effects of Screw Configuration, Temperature Profile, and Devulcanization Agent Concentration.
- [39] Kojima, M., Tosaka, M., and Ikeda, Y. (2004). Chemical recycling of sulfur-cured natural rubber using supercritical carbon dioxide. *Green Chemistry*, 6(2), 84.
- [40] Kojima, M., Kohjiya, S., and Ikeda, Y. (2005). Role of supercritical carbon dioxide for selective impregnation of decrosslinking reagent into isoprene rubber vulcanizate. *Polymer*, 46(7), 2016–2019.
- [41] Kojima, M., Tosaka, M., Ikeda, Y., and Kohjiya, S. (2005). Devulcanization of carbon black filled natural rubber using supercritical carbon dioxide. *Journal of Applied Polymer Science*, 95(1), 137–143.
- [42] Tzoganakis, C. (2007). *U.S. Patent No. 7,189,762*. Washington, DC: U.S. Patent and Trademark Office.

- [43] Tzoganakis, C., and Zhang, Q. (2004). Devulcanization of recycled tire rubber using supercritical carbon dioxide. In *ANTEC-CONFERENCE PROCEEDINGS*-(Vol. 3, pp. 3509-3513): Society of Plastic Engineers.
- [44] Meysami, M., and Tzoganakis, C. Continuous Rubber Devulcanization Using Supercritical Co<sub>2</sub>: Recycling Tire Rubber Crumb. In *8th World Congress of Chemical Engineering*.
- [45] Meysami, M., Mutyala, P., Zhu, S., and Tzoganakis, C. (2013). Effect of process parameters on properties of devulcanized rubber obtained from a supercritical CO<sub>2</sub> assisted devulcanization process. In *ANTEC-CONFERENCE PROCEEDINGS*:Society of Plastic Engineers.
- [46] Meysami, M., and Tzoganakis, C. (2008). Devulcanization of recycled tire rubber crumb with supercritical co<sub>2</sub>: curing behavior, mechanical properties and degree of devulcanization process. In *ANTEC-CONFERENCE PROCEEDINGS*:Society of Plastic Engineers.
- [47] Nicula, R. (2002). *Introduction to differential scanning calorimetry*. Course, Rostock, Germany: Rostock University.
- [48] Lukas, K., and LeMaire, P. K. (2009). Differential scanning calorimetry: fundamental overview. *Resonance*, 14(8), 807-817. Central Connecticut State University, New Britain.
- [49] Cooper, A., Nutley, M. A., and Wadood, A. (2000). Differential scanning microcalorimetry. Protein-ligand interactions: *Hydrodynamics and Calorimetry*, 287-318.
- [50] Isayev, A. I., and Sujan, B. (2006). Nonisothermal vulcanization of devulcanized GRT with reversion type behavior. *Journal of Elastomers and Plastics*, 38(4), 291-318.
- [51] Arrillaga, A., Zaldua, A. M., Atxurra, R. M., and Farid, A. S. (2007). Techniques used for determining cure kinetics of rubber compounds. *European Polymer Journal*, 43(11), 4783-4799.

- [52] Halley, P. J., and Mackay, M. E. (1996). Chemorheology of thermosets—an overview. *Polymer Engineering and Science*, 36(5), 593-609.
- [53] Ding, R., and Leonov, A. I. (1996). A kinetic model for sulfur accelerated vulcanization of a natural rubber compound. *Journal of Applied Polymer Science*, 61(3), 455-463.
- [54] Ding, R., Leonov, A. I., and Coran, A. Y. (1996). A study of the vulcanization kinetics of an accelerated-sulfur SBR compound. *Rubber Chemistry and Technology*, 69(1), 81-91.
- [55] Fan, R. L., Zhang, Y., Huang, C., Gong, P., and Zhang, Y. X. (2002). Simulation and verification for sulfur accelerated vulcanization of gum natural rubber compound. *Rubber Chemistry and Technology*, 75(2), 287-297.
- [56] Kamal, M. R., and Sourour, S. (1973). Kinetics and thermal characterization of thermoset cure. *Polymer Engineering and Science*, 13(1), 59-64.
- [57] Kamal, M. R. (1974). Thermoset characterization for moldability analysis. *Polymer Engineering and Science*, 14(3), 231-239.
- [58] Karkanias, P. I., Partridge, I. K., and Attwood, D. (1996). Modelling the cure of a commercial epoxy resin for applications in resin transfer moulding. *Polymer International*, 41(2), 183-191.
- [59] Chough, S. H., and Chang, D. H. (1996). Kinetics of sulfur vulcanization of NR, BR, SBR, and their blends using a rheometer and DSC. *Journal of Applied Polymer Science*, 61(3), 449-454.
- [60] Isayev, A. I., and Deng, J. S. (1988). Nonisothermal vulcanization of rubber compounds. *Rubber Chemistry and Technology*, 61(2), 340-361.

- [61] Khang, T. H., and Ariff, Z. M. (2012). Vulcanization kinetics study of natural rubber compounds having different formulation variables. *Journal of Thermal Analysis and Calorimetry*, 109(3), 1545-1553.
- [62] Mansilla, M. A., and Marzocca, A. J. (2012). About the cure kinetics in natural rubber/styrene Butadiene rubber blends at 433K. *Physica B: Condensed Matter*, 407(16), 3271-3273.
- [63] Hong, I. K., and Lee, S. (2013). Cure kinetics and modeling the reaction of silicone rubber. *Journal of Industrial and Engineering Chemistry*, 19(1), 42-47.
- [64] Hernandez-Ortiz, J. P., and Osswald, T. A. (2005). A novel cure reaction model fitting technique based on DSC scans. *Journal of Polymer Engineering*, 25(1), 23-38.
- [65] Lopez, L. M., Cosgrove, A. B., Hernandez-Ortiz, J. P., and Osswald, T. A. (2007). Modeling the vulcanization reaction of silicone rubber. *Polymer Engineering and Science*, 47(5), 675-683.
- [66] Kissinger, H. E. (1956). Variation of peak temperature with heating rate in differential thermal analysis. *Journal of Research of the National Bureau of Standards*, 57(4), 217-221.
- [67] Kissinger, H. E. (1957). Reaction kinetics in differential thermal analysis. *Analytical Chemistry*, 29(11), 1702-1706.
- [68] Laidler, K. J. (1984). The development of the Arrhenius equation. *Journal of Chemical Education*, 61, 494.
- [69] Coran, A.Y. (1964). Paper no.22, presented to *Division of Rubber Chemistry, A.C.S., Chicago*.
- [70] Mutyala, P. (2013). Preparation of Thermoplastic Vulcanizates from Devulcanized Rubber and Polypropylene. Doctoral dissertation, University of Waterloo.